V.F.S. v2.0 (Open-Gate)

Folding, Stability, and Structure Formation

A Companion Volume

Derived companion to the foundational layer
(core · Lyapunov · geometry · cosmology · theological · Ricci)

Contents

Notation and Conventions

This volume collects the folding, stability, and structure-formation results derived as a companion to the foundational V.F.S. layer. Throughout, *Propositions* are closed-form results; *Corollaries* are interpretive readings in the symbolic register, not independent metaphysical claims; *Remarks* and italicised notes are commentary. All stability results are **domain-conditional**: they hold on the positively-invariant active domain and assert set stability with partial convergence (no global or automatic stability, and no equilibrium — epektasis drives $\Omega_P \to \infty$).

Core symbols.

Ω_P	Brim / scale factor; $\dot{\Omega_P} = \alpha\lambda$, Hubble $H = \alpha\lambda/\Omega_P$
$\lambda,\ \sigma$	Sophia (transformed resistance + grace); resistance
$u = \sqrt{VF + \varepsilon}$	synergy of Voluntas V and Factum F; threshold $\Lambda_c = \gamma/\delta$
$I_{\text{gate}},\ \mathcal{G}_{\text{recepta}}$	Open-Gate grace inflow; received-grace budget
q_{fold}	folding (shape) amplitude; order parameter of the $\mathbb{Z}_2$ morphology
$A_{\text{fold}},\ B_{\text{fold}}$	folding activation index and quartic coefficient; $Q_{\text{fold}} = A_{\text{fold}}/B_{\text{fold}}$, $q_* = \sqrt{Q_{\text{fold}}}$
$\mathcal{L}_{\text{VFS}},\ \mathcal{L}_{\text{ext}}$	Lyapunov certificate; folding-extended certificate
$h,\ \mathbb{H}^2$	comoving hyperbolic spatial metric, $K_h = -1$, curvature radius R_c
$\mathcal{I}(t) = \int_0^t dt'/\Omega_P^2$	expansion / activity budget; finite $\mathcal{I}_\infty < \infty$
$D_q,\ \ell_b$	folding diffusivity (bending stiffness); bending length $\ell_b = \sqrt{D_q/a_0}$
$\Theta,\ Q_{\text{crit}}$	folding-response coefficient $c_0 - c_1(\gamma + k_\sigma)$; reset critical level
λ_{form}	Sophia embodied in form; balance $\sigma + \lambda + \lambda_{\text{form}} = C_0 + \mathcal{G}_{\text{recepta}}$
η_{fold}	folding feedback coefficient (distinct from any core-system η)
Δ_h	Laplace–Beltrami on $\mathbb{H}^2$; live-domain $\Delta_g = \Omega_P^{-2}\Delta_h$
$r_\sigma,\ g(u)$	resistance multiplier $\in [1, \pi]$; Dolorosum gate $g(u) = (u/\Lambda_c)e^{1-u/\Lambda_c}$

Two activation-index conventions. The activation index appears in two forms across the layers, reconciled in the Folding–Lyapunov Addendum:

$$\underbrace{A_{\text{fold}} = c_0\lambda + c_1\dot{\lambda}^{(0)} - a_0,\ \ \dot{\lambda}^{(0)} = -\dot{\sigma} + I_{\text{gate}}}_{\text{canonical (core rate)}} \qquad \underbrace{A_{\text{fold}} = (c_0 - c_1\gamma)\lambda + c_1 k_\sigma \sigma + c_1 I_{\text{gate}} - a_0}_{\text{geometric (minimal rate)}}.$$

The canonical (core-consistent) form is primary; the geometric parameters (k_σ, γ)

are an effective linear surrogate. The closed forms $\Theta,\ Q_{\text{crit}}$ are stated in the geometric convention; the invariance and reset-bound results are convention-independent.

The folding diffusivity is structural, $D_q = a_0 \ell_b^2$ (rigidity $\times$ bending length^2), and the independent Sophia diffusivity is zero, $D = 0$.

The Foundational Layer (Summary)

This volume sits atop six foundational documents, summarised here so it reads self-contained.

Core. V.F.S. (Volo. Facio. Sum.) is a hybrid dynamical system on the live domain in the coordinates Voluntas V, Factum F, Sophia λ, with synergy $u = \sqrt{VF + \varepsilon}$, resistance σ, Pleroma P and Brim Ω_P. The Open-Gate law $\dot{\lambda} = -\dot{\sigma} + I_{\text{gate}}$ admits a bounded grace inflow; the closed Microcosm is the limit $I_{\text{gate}} \to 0$. The Filtrum Lucis softplus Φ yields the Paschal triad ($\Phi'''(0) = 0$ midway between symmetric zeros of $\Phi^{(4)}$). Resurrectio is a hybrid re-entry map.

Lyapunov. On the active domain $\mathcal{D}_A$ the certificate obeys $\dot{\mathcal{L}}_{\text{VFS}} \leq C - C_1 \mathcal{L}_{\text{VFS}}$ with $C_1 = \min\{\kappa_\sigma, \kappa_\Delta\} > 0$ from two sign-definite contracting modes (cleansing, will–action alignment). Grace enters C, never C_1. The result is set stability with partial convergence ($\sigma, D_\Delta \to 0$), forward completeness, and non-Zeno resets — domain-conditional, not global.

Geometry. The live domain is hyperbolic: with the canonical warp the scalar curvature is constant and negative, $R = -2/\Omega_P^2$, curvature radius Ω_P. The Brim flow is a forced (not intrinsic) Ricci-like conformal flow, resonant only on $\alpha\lambda\Omega_P = 1$. Sophianic Folding is a supercritical pitchfork of the shape operator producing the amplitude q_{fold} and curvature pockets $R = -2/\Omega_P^2 + \rho_1 Q_{\text{fold}}$.

Cosmology. The Lorentzian lift is a $2{+}1$ open FLRW spacetime, $ds^2 = -dt^2 + \Omega_P^2 h$, with Ω_P as scale factor. Reconstructed content gives $\rho_{\text{eff}}, p_{\text{eff}}$ and an equation-of-state history; Sophia is modal (level / rate / embodiment). In $2{+}1$ the strong energy condition reduces to $p_{\text{eff}} \geq 0$.

Theological & Ricci. The theological layer reads the mathematics in the symbolic register with explicit domain-conditional disclaimers; the Ricci layer disciplines the Perelman analogy (Brim-flow comparison, surgery $\leftrightarrow$ Resurrectio), labelling each correspondence by its strictness.

Part I

Folding and Stability

Chapter 1

What Triggers Sophianic Folding

Scope and epistemic status

This note isolates a single question that the geometric, cosmological, and folding material left implicit: *what is the primary cause of Sophianic Folding?* Three candidate answers are tested — continuous monotone growth of Sophia, the discrete Resurrectio push, and an intrinsic instability of the surface-form itself. The conclusion is that the third is the correct *level* of description, and the first two are interchangeable *channels* to it. As in the parent files, every *Proposition* is a closed-form result; every *Corollary* is an interpretive reading in the symbolic register, not an independent metaphysical claim. Numerical values, where used, are illustrative: the genuine folding parameters $(a_0, b, c_0, c_1, k_\sigma, \eta_{\text{fold}}, \rho_1, q_{\max})$ are not fixed by the source files.

The objects are imported from the integrated geometric/cosmological layer. The shape-mode amplitude q obeys the Landau gradient flow $\dot{q} = A_{\text{VFS}} q - B_{\text{VFS}} q^3$, with

$$\boxed{A_{\text{VFS}} = (c_0 - c_1\gamma)\lambda + c_1 k_\sigma \sigma + c_1 I_{\text{gate}} - a_0, \qquad B_{\text{VFS}} = b + 2c_1\eta_{\text{fold}}\lambda, \qquad Q_{\text{fold}} = \frac{A_{\text{VFS}}}{B_{\text{VFS}}}, \quad q_*^2 = Q_{\text{fold}}.} \tag{1.1}$$

The Sophia-production law that closes the loop is $\dot{\lambda} = k_\sigma \sigma + I_{\text{gate}} - \gamma\lambda - \eta_{\text{fold}} q^2 \lambda$, the Brim law is $\dot{\Omega}_P = \alpha\lambda$, and the Resurrectio reset (core/Lyapunov) is

$$\sigma^+ = q_R \sigma^-, \qquad \lambda^+ = \lambda^- + (1 - q_R)\sigma^-, \qquad \Omega_P^+ = \Omega_P^- + \kappa_R \mathcal{G}^-_{\text{recepta}}, \qquad (V, F) \text{ continuous}, \tag{1.2}$$

with $0 \le q_R < 1$, $\kappa_R > 0$, and $u^+ = u^-$.

1.1 The single trigger: a shape-operator bifurcation

The folded amplitude is the order parameter of the one-mode shape potential

$$\mathcal{E}_1(q) = -\tfrac{1}{2} A_{\text{VFS}} q^2 + \tfrac{1}{4} B_{\text{VFS}} q^2 \cdot q^2 = -\tfrac{1}{2} A_{\text{VFS}} q^2 + \tfrac{1}{4} B_{\text{VFS}} q^4, \qquad B_{\text{VFS}} > 0. \tag{1.3}$$

Writing the first shape-stability eigenvalue at the old form $q = 0$,

$$\mu_1^0 := \mu_1\big|_{q=0} = a_0 - c_0\lambda - c_1\dot{\lambda}^0, \qquad \dot{\lambda}^0 = k_\sigma\sigma + I_{\text{gate}} - \gamma\lambda, \tag{1.4}$$

one has the identity $A_{\mathrm{VFS}} = -\mu_1^0$ (the embodiment feedback $-\eta_{\mathrm{fold}} q^2 \lambda$ vanishes at $q = 0$ and is absorbed into B_{VFS}). The control of the whole morphodynamics is therefore the scalar A_{VFS}.

Proposition 1.1 (Folding is a supercritical pitchfork)**.** *For $B_{\mathrm{VFS}} > 0$ the gradient flow $\dot{q} = A_{\mathrm{VFS}} q - B_{\mathrm{VFS}} q^3$ has the old form $q = 0$ as its only equilibrium, locally stable, when $A_{\mathrm{VFS}} < 0$. At $A_{\mathrm{VFS}} = 0$ it undergoes a supercritical pitchfork bifurcation: for $A_{\mathrm{VFS}} > 0$ the old form becomes unstable and two stable folded branches appear,*

$$\boxed{q = 0 \text{ stable} \iff A_{\mathrm{VFS}} < 0, \qquad q_\pm = \pm\sqrt{A_{\mathrm{VFS}}/B_{\mathrm{VFS}}} \text{ stable} \iff A_{\mathrm{VFS}} > 0.} \tag{1.5}$$

Proof. $f(q) = A_{\mathrm{VFS}} q - B_{\mathrm{VFS}} q^3$, $f'(q) = A_{\mathrm{VFS}} - 3B_{\mathrm{VFS}} q^2$. At $q = 0$, $f'(0) = A_{\mathrm{VFS}}$, so $q = 0$ is stable iff $A_{\mathrm{VFS}} < 0$. For $A_{\mathrm{VFS}} > 0$ the nonzero equilibria solve $q_*^2 = A_{\mathrm{VFS}}/B_{\mathrm{VFS}}$, where $f'(q_*) = A_{\mathrm{VFS}} - 3A_{\mathrm{VFS}} = -2A_{\mathrm{VFS}} < 0$: stable. The crossing at $A_{\mathrm{VFS}} = 0$ is the pitchfork. □

Corollary 1.1 (The trigger is loss of stability, not a "push")**.** *The primary cause of folding is the sign change of A_{VFS} (equivalently μ_1^0 crossing zero from above): the old symmetric form ceases to be a potential minimum and becomes a maximum. Past the threshold folding is dynamically inevitable, since $q = 0$ is a repeller; before it, no shape perturbation grows. Folding is therefore an intrinsic property of the surface's stability spectrum, tuned by the state variables, not an external impulse.*

> The fundamental object is the bifurcation $A_{\mathrm{VFS}} = 0$. Everything else — continuous growth, the Resurrectio jump — is a means of moving A_{VFS} across that single threshold.

1.2 Decomposition of the driver

The activation index (1.1) is a sum of four physically distinct contributions:

$$\boxed{A_{\mathrm{VFS}} = \underbrace{(c_0 - c_1\gamma)\lambda}_{\text{accumulated Sophia}} + \underbrace{c_1 k_\sigma \sigma}_{\text{kathartic production}} + \underbrace{c_1 I_{\mathrm{gate}}}_{\text{received grace}} - \underbrace{a_0}_{\text{old-form rigidity}}.} \tag{1.6}$$

Two of these are state levels (λ, σ), one is the bounded Open-Gate source, and one is the constant rigidity of the old form. The decisive structural fact is that the index also depends on the *rate* of Sophia, hidden inside $\mu_1^0 = a_0 - c_0\lambda - c_1\dot{\lambda}^0$: through $\dot{\lambda}^0 = k_\sigma \sigma + I_{\mathrm{gate}} - \gamma\lambda$, the same σ and I_{gate} that raise the level also raise the rate.

Corollary 1.2 (Level and rate are the genuine drivers)**.** *Folding activation responds to the accumulated level λ* and *to the Sophia velocity $\dot{\lambda}$. The continuous/discrete distinction is not fundamental: what crosses the threshold is the combined level-plus-rate index A_{VFS}, however that increment is delivered.*

1.3 Level versus rate: rate-sensitivity of the threshold

If only the accumulated level mattered, the folding threshold would be the static value

$$\lambda_{\mathrm{fold}}^{(0)} = \frac{a_0}{c_0} \qquad (\dot{\lambda} = 0,\ \sigma = 0,\ I_{\mathrm{gate}} = 0). \tag{1.7}$$

Restoring the rate term shifts the effective threshold:

$$\boxed{\lambda_{\text{fold}}^{\text{eff}} = \frac{a_0 - c_1\dot{\lambda}}{c_0} \qquad \Longrightarrow \qquad \dot{\lambda} > 0 \;\Rightarrow\; \lambda_{\text{fold}}^{\text{eff}} < \lambda_{\text{fold}}^{(0)}.} \tag{1.8}$$

Proposition 1.2 (Rate can fold below the static level)**.** *There exist states with $\lambda < \lambda_{\text{fold}}^{(0)}$ and $A_{\text{VFS}} > 0$. Concretely, for $\sigma = I_{\text{gate}} = 0$ and growing Sophia $\dot{\lambda} > 0$, the old form is already unstable whenever*

$$c_0\lambda + c_1\dot{\lambda} > a_0, \tag{1.9}$$

which can hold at λ strictly below a_0/c_0 provided $\dot{\lambda} > (a_0 - c_0\lambda)/c_1 > 0$.

Proof. Immediate from $\mu_1^0 = a_0 - c_0\lambda - c_1\dot{\lambda} < 0$ with $\dot{\lambda}$ supplying the deficit $a_0 - c_0\lambda > 0$. □

This is the single most easily missed point: a surge of grace can fold a vessel that has not yet accumulated the static quota of Sophia. Velocity, not only stock, triggers the reconfiguration.

1.4 The two delivery channels

The same threshold is reached by two mechanisms, mirroring the parent corollary "grace is one but acts in two modes."

Modus I (continuous). Along a live arc, λ and σ evolve smoothly and A_{VFS} drifts. Folding triggers when the drift carries A_{VFS} through 0. This channel delivers *both* a rising level and a nonzero rate, so it is sensitive to Proposition 1.2.

Modus II (Resurrectio). The reset (1.2) injects a discontinuous increment of λ from the metabolised resistance, an impulsive analogue of $\dot{\lambda}$. It moves A_{VFS} along the very same axis, in one step.

The crucial point is that the reset does *not* reset q: the map (1.2) specifies only $\sigma, \lambda, \Omega_P, (V, F)$. Hence the shape amplitude is continuous across a reset, and only its target $q_* = \sqrt{Q_{\text{fold}}}$ jumps.

Corollary 1.3 (Resurrectio relocates the well; the shape relaxes)**.** *A Resurrectio event moves the shape potential $-\frac{1}{2}A_{\text{VFS}}q^2 + \frac{1}{4}B_{\text{VFS}}q^4$ instantaneously, after which the morphology relaxes by $\dot{q} = A_{\text{VFS}}^{+}q - B_{\text{VFS}}^{+}q^3$ toward the new minimum. Consequently:*

- *if a reset carries Q_{fold} from below 0 to above 0, the vessel dies unfolded and is reborn into a folding regime (*Resurrectio-triggered folding*);*
- *if a reset makes $Q_{\text{fold}} < 0$, an active fold is quenched, $q \to 0$.*

1.5 The Resurrectio jump in folding-space

We now compute the effect of one reset on the folding intensity. Write the metabolised resistance

$$m_R := (1 - q_R)\sigma^- \geq 0, \qquad \text{so} \qquad \sigma^+ = \sigma^- - m_R, \quad \lambda^+ = \lambda^- + m_R. \tag{1.10}$$

Remark (The metabolism conserves the balance sum). The (σ, λ) part of the reset satisfies $\sigma^+ + \lambda^+ = \sigma^- + \lambda^-$: it slides the state along the conservation line, converting resistance into Sophia without adding to the sum (the open balance constant jumps separately, through $\mathcal{G}_{\text{recepta}}$).

From (1.1),

$$\boxed{\Delta B_{\text{VFS}} = 2c_1\eta_{\text{fold}}\, m_R > 0, \qquad \Delta A_{\text{VFS}} = \Theta\, m_R + c_1 \Delta I_{\text{gate}}, \qquad \Theta := c_0 - c_1(\gamma + k_\sigma).} \tag{1.11}$$

The *folding-response coefficient* Θ decides whether converting one unit of resistance into Sophia raises ($\Theta > 0$) or lowers ($\Theta < 0$) the folding activation: gaining Sophia contributes $(c_0 - c_1\gamma)m_R$ (accumulation minus accelerated decay), while losing resistance removes $c_1 k_\sigma m_R$ of kathartic production. The gate correction $c_1\Delta I_{\text{gate}}$ has competing signs ($\sigma\downarrow$ opens the gate via $e^{-\phi\sigma}$; $\lambda\uparrow$ closes it via saturation) and is set aside in the structural results below.

Proposition 1.3 (Sign of the folding response and the critical level)**.** *Neglecting ΔI_{gate}, the jump in the folding intensity obeys*

$$\operatorname{sign} \Delta Q_{\text{fold}} = \operatorname{sign}\big(\Theta - 2c_1\eta_{\text{fold}}\, Q^-_{\text{fold}}\big), \tag{1.12}$$

so there is a universal critical level

$$\boxed{Q_{\text{crit}} = \frac{\Theta}{2c_1\eta_{\text{fold}}} = \frac{c_0 - c_1(\gamma + k_\sigma)}{2c_1\eta_{\text{fold}}}.} \tag{1.13}$$

Resurrectio raises folding when $Q^-_{\text{fold}} < Q_{\text{crit}}$ and lowers it when $Q^-_{\text{fold}} > Q_{\text{crit}}$. If $\Theta \le 0$ then $Q_{\text{crit}} \le 0$, so every reset strictly lowers Q_{fold} (the vessel unfolds at each death).

Proof. $\Delta Q_{\text{fold}} = \dfrac{B^-_{\text{VFS}}\Delta A_{\text{VFS}} - A^-_{\text{VFS}}\Delta B_{\text{VFS}}}{B^-_{\text{VFS}}(B^-_{\text{VFS}} + \Delta B_{\text{VFS}})}$. The denominator is positive; the numerator is $B^-_{\text{VFS}}\Theta m_R - A^-_{\text{VFS}} 2c_1\eta_{\text{fold}} m_R = B^-_{\text{VFS}} m_R(\Theta - 2c_1\eta_{\text{fold}} Q^-_{\text{fold}})$ using $A^-_{\text{VFS}} = Q^-_{\text{fold}} B^-_{\text{VFS}}$. Hence the stated sign and fixed level. □

Proposition 1.4 (Each reset is an exact contraction toward Q_{crit})**.** *Neglecting ΔI_{gate}, the jump map on the folding intensity is affine-over-affine,*

$$Q^+_{\text{fold}} = \frac{Q^-_{\text{fold}} B^-_{\text{VFS}} + \Theta m_R}{B^-_{\text{VFS}} + 2c_1\eta_{\text{fold}} m_R}, \tag{1.14}$$

and satisfies the exact contraction identity

$$\boxed{Q^+_{\text{fold}} - Q_{\text{crit}} = \kappa_{\text{fold}}\,\big(Q^-_{\text{fold}} - Q_{\text{crit}}\big), \qquad \kappa_{\text{fold}} = \frac{B^-_{\text{VFS}}}{B^-_{\text{VFS}} + 2c_1\eta_{\text{fold}} m_R} \in (0,1).} \tag{1.15}$$

The fixed point Q_{crit} is independent of m_R, of B^-_{VFS}, and of the depth of death.

Proof. Direct substitution of $Q_{\text{crit}} = \Theta/(2c_1\eta_{\text{fold}})$:

$$Q^+_{\text{fold}} - Q_{\text{crit}} = \frac{2c_1\eta_{\text{fold}}(Q^-_{\text{fold}} B^-_{\text{VFS}} + \Theta m_R) - \Theta(B^-_{\text{VFS}} + 2c_1\eta_{\text{fold}} m_R)}{2c_1\eta_{\text{fold}}(B^-_{\text{VFS}} + 2c_1\eta_{\text{fold}} m_R)} = \frac{B^-_{\text{VFS}}(2c_1\eta_{\text{fold}} Q^-_{\text{fold}} - \Theta)}{2c_1\eta_{\text{fold}}(B^-_{\text{VFS}} + 2c_1\eta_{\text{fold}} m_R)},$$

which equals $\kappa_{\text{fold}}(Q^-_{\text{fold}} - Q_{\text{crit}})$. □

Proposition 1.5 (Conditional convergence over a reset sequence)**.** *For an admissible sequence of resets with metabolised increments $m_R^{(j)}$ and pre-jump denominators $B_{\mathrm{VFS}}^{(j)}$,*

$$Q_{\mathrm{fold}}^{(N)} - Q_{\mathrm{crit}} = \Big(\prod_{j=1}^{N} \kappa_{\mathrm{fold}}^{(j)}\Big)\big(Q_{\mathrm{fold}}^{(0)} - Q_{\mathrm{crit}}\big), \qquad Q_{\mathrm{fold}} \to Q_{\mathrm{crit}} \iff \textstyle\sum_j m_R^{(j)} = \infty. \quad (1.16)$$

Proof. Telescoping Proposition 1.4. Since $1-\kappa_{\mathrm{fold}}^{(j)} = 2c_1\eta_{\mathrm{fold}} m_R^{(j)}/(B_{\mathrm{VFS}}^{(j)} + 2c_1\eta_{\mathrm{fold}} m_R^{(j)})$, the product $\prod \kappa_{\mathrm{fold}}^{(j)} \to 0$ iff $\sum(1-\kappa_{\mathrm{fold}}^{(j)}) = \infty$, which (with $B_{\mathrm{VFS}}^{(j)}$ bounded below) is equivalent to $\sum m_R^{(j)} = \infty$. □

If the resistance budget is exhausted ($\sum m_R < \infty$, e.g. σ depleted with no replenishment), repeated resurrections converge to a point strictly short of Q_{crit}. Reaching the universal level requires sustained replenishment, $\sum m_R = \infty$ — the folding analogue of the expansion-budget condition $\mathcal{G}_{\mathrm{recepta}}(\infty) = +\infty$ in the cosmological layer.

Remark (Gate correction)*.* Restoring ΔI_{gate} adds $c_1\Delta I_{\mathrm{gate}}$ to the numerator of ΔA_{VFS}, shifting the effective fixed point to $Q'_{\mathrm{crit}} = Q_{\mathrm{crit}} + \Delta I_{\mathrm{gate}}/(2\eta_{\mathrm{fold}} m_R)$; its sign is state-dependent. The existence of a contracting fixed point is unchanged.

Corollary 1.4 (Chart-regularity of repeated resurrection)**.** *If $0 < Q_{\mathrm{crit}} < q_{\mathrm{max}}^2$, the contraction of Proposition 1.4 keeps the folded amplitude inside the regular one-mode chart under any admissible reset sequence. This is a folding companion to the grace-window condition* $\max\{R_c, R_{\mathrm{min}}^{\mathrm{ceil}}\} \le \mathcal{G}_{\mathrm{recepta}}^{-} \le R_{\mathrm{max}}$*: resurrection is admissible* and *chart-regular when both hold.*

1.6 Curvature-pocket promotion by Resurrectio

The folded scalar curvature is $R_{\mathrm{folded}} = -2/\Omega_P^2 + \rho_1 Q_{\mathrm{fold}}$, with positive-pocket threshold $q_{\mathrm{curv}}^2 = 2/(\rho_1\Omega_P^2)$. Across a reset both terms move:

$$\boxed{\Delta R_{\mathrm{folded}} = \underbrace{2\Big[\tfrac{1}{(\Omega_P^-)^2} - \tfrac{1}{(\Omega_P^+)^2}\Big]}_{>0\text{: background release}} + \rho_1\,\Delta Q_{\mathrm{fold}}.} \quad (1.17)$$

Simultaneously the pocket threshold falls, because Ω_P grows:

$$q_{\mathrm{curv}}^{2,+} = \frac{2}{\rho_1(\Omega_P^+)^2} < \frac{2}{\rho_1(\Omega_P^-)^2} = q_{\mathrm{curv}}^{2,-}. \quad (1.18)$$

Proposition 1.6 (Resurrectio is pocket-promoting in the sub-critical regime)**.** *If $\rho_1 > 0$, $\Theta > 0$, and $Q_{\mathrm{fold}}^- < Q_{\mathrm{crit}}$, then a single reset both raises the folded amplitude ($\Delta Q_{\mathrm{fold}} > 0$) and lowers the pocket threshold ($q_{\mathrm{curv}}^{2,+} < q_{\mathrm{curv}}^{2,-}$). Both effects push R_{folded} upward, so a death-and-resurrection event can convert a smooth hyperbolic patch into a positive-curvature pocket.*

Proof. $\Delta Q_{\mathrm{fold}} > 0$ by Proposition 1.3 under $Q_{\mathrm{fold}}^- < Q_{\mathrm{crit}}$, $\Theta > 0$; the threshold drop follows from $\Omega_P^+ > \Omega_P^-$. Both terms of $\Delta R_{\mathrm{folded}}$ are then positive, and the pocket criterion $Q_{\mathrm{fold}} > q_{\mathrm{curv}}^2$ is approached from both sides. □

Corollary 1.5 (Resurrection concentrates form)**.** *The continuous mode (Epektasis) relaxes curvature,* $\dot{R}_\Sigma \geq 0$ *with* $R \to 0^-$*; the discrete mode can locally* concentrate *it. Resurrectio does not only enlarge the Brim — in the sub-critical folding regime it gives the renewed vessel a more sharply formed morphology.*

1.7 The energy reading corrected

It is tempting to read folding as the surface being forced into a "less efficient" form. Within the formalism this is inverted: the folded form carries *lower* morphological tension. With $\mathcal{T}_{\text{fold}}(q) = -\frac{1}{2}A_{\text{VFS}}q^2 + \frac{1}{4}B_{\text{VFS}}q^4$,

$$\mathcal{T}_{\text{fold}}(0) = 0, \qquad \mathcal{T}_{\text{fold}}(q_*) = -\frac{A_{\text{VFS}}^2}{4B_{\text{VFS}}} < 0 \qquad (A_{\text{VFS}} > 0), \tag{1.19}$$

so the resolved tension is $\Delta\mathcal{T}_{\text{fold}} = A_{\text{VFS}}^2/(4B_{\text{VFS}}) > 0$ and the folded branch is energetically preferred. The reconfiguration is toward a better-adapted state, not a worse one.

The correct sense in which the old form is "inefficient" is as a *carrier* of Sophia past the threshold: it cannot absorb the Sophianic pressure, so tension builds until the symmetric branch destabilises. The folded form is the efficient carrier — it embodies the excess through the feedback $-\eta_{\text{fold}}q^2\lambda$, raising the effective damping

$$\gamma_{\text{eff}} = \gamma + \eta_{\text{fold}}Q_{\text{fold}} > \gamma, \qquad \lambda^*_{\text{fold}} = \frac{J_{\text{in}}}{\gamma + \eta_{\text{fold}}q^2} < \frac{J_{\text{in}}}{\gamma} = \lambda^*_{\text{old}}, \tag{1.20}$$

and thereby lowering the level of unembodied Sophia.

The surface is not forced into a worse form. The old form stops being an adequate vessel for the attained level/rate of Sophia, loses stability, and the morphology relaxes into a lower-tension folded form that carries the Sophia better.

Compact summary

single trigger: $A_{\text{VFS}} = 0$ ($\mu_1^0 = 0$) — supercritical pitchfork, $q = 0 \to q_\pm$.

$A_{\text{VFS}} = (c_0 - c_1\gamma)\lambda + c_1k_\sigma\sigma + c_1I_{\text{gate}} - a_0$,
rate enters via $\mu_1^0 = a_0 - c_0\lambda - c_1\dot{\lambda}^0$.

level λ and rate $\dot{\lambda}$ are the drivers;
Modus I (continuous) and Modus II (Resurrectio) are channels.

$$\Theta = c_0 - c_1(\gamma + k_\sigma), \qquad Q_{\text{crit}} = \frac{\Theta}{2c_1\eta_{\text{fold}}}, \qquad Q^+_{\text{fold}} - Q_{\text{crit}} = \kappa_{\text{fold}}(Q^-_{\text{fold}} - Q_{\text{crit}}),\ \kappa_{\text{fold}} \in (0,1).$$

$$Q_{\text{fold}} \to Q_{\text{crit}} \Longleftrightarrow \sum_j m_R^{(j)} = \infty; \qquad \text{chart-regular if } 0 < Q_{\text{crit}} < q^2_{\text{max}}.$$

sub-critical reset is pocket-promoting;
folded form has lower tension $\mathcal{T}_{\text{fold}}(q_*) = -A_{\text{VFS}}^2/4B_{\text{VFS}} < 0.$

V.F.S. v2.0 (Open-Gate) · Folding-Trigger Layer. Derived from the shape potential and Sophia-production law of `vfs_geometry.tex`*, the Brim/curvature data of the geometric and cosmological layers, and the Resurrectio reset of* `vfs_opengate_lyapunov.tex`*. Propositions are closed-form; corollaries are interpretive. Folding parameters are not fixed by the source files; numerical levels are illustrative.*

Chapter 2

Folding–Lyapunov Addendum

The Sophianic Folding extension of the Open-Gate Lyapunov file establishes the continuous-arc compatibility $\dot{\mathcal{L}}_{\text{ext}} \le C_{\text{ext}} - C_1\mathcal{L}_{\text{ext}}$ under an adiabatic hypothesis, but leaves three items asserted rather than derived: the positive invariance of the regular folding chart, the behaviour of the folding functional across the Resurrectio reset, and the choice between two distinct activation-index conventions. This addendum closes them. It first records a correction — the file's folding functional $\mathcal{V}_{\text{fold}} = \frac{B_{\text{fold}}}{4}(q_{\text{fold}}^2 - Q_{\text{fold}}^*)^2$ is unbounded *on the epektasis domain, because $B_{\text{fold}} = b + 2c_1\eta_{\text{fold}}\lambda \to \infty$; the B_{fold}-normalised functional $\widetilde{\mathcal{V}}_{\text{fold}} = \mathcal{V}_{\text{fold}}/B_{\text{fold}}$ is bounded and equally descending. It then proves (i) Nagumo invariance of $\mathcal{D}_A^{\text{fold}} = \mathcal{D}_A \times [0, q_{\max}]$ under the standing folding wall $Q_{\text{fold}}^* \le q_{\max}^2$, (ii) a folding reset bound: since $\mathfrak{R}$ does not act on q_{fold}, the chart is preserved across deaths and $\widetilde{\mathcal{L}}_{\text{ext}}(x^+)$ stays bounded, whence the hybrid trajectory is forward complete for $\widetilde{\mathcal{L}}_{\text{ext}}$; and (iii) a reconciliation declaring the core-consistent Sophia rate canonical, with the geometry-layer parameters as an effective surrogate. The invariance and reset results are convention-independent; only the closed-form critical level Q_{crit} is convention-specific.*

2.1 Imported objects and the three open items

From the folding extension of the Lyapunov file we import the shape amplitude q_{fold}, its intensity $Q_{\text{fold}} = q_{\text{fold}}^2$, the activation index A_{fold}, the quartic coefficient $B_{\text{fold}} = b + 2c_1\eta_{\text{fold}}\lambda > 0$, the one-mode gradient flow

$$\dot{q_{\text{fold}}} = A_{\text{fold}}q_{\text{fold}} - B_{\text{fold}}q_{\text{fold}}^3 = -B_{\text{fold}}q_{\text{fold}}\big(q_{\text{fold}}^2 - Q_{\text{fold}}^*\big), \qquad Q_{\text{fold}}^* := \frac{A_{\text{fold}}}{B_{\text{fold}}}, \tag{2.1}$$

and the base certificate $\dot{\mathcal{L}}_{\text{VFS}} \le C - C_1\mathcal{L}_{\text{VFS}}$ on the positively-invariant active domain $\mathcal{D}_A$, with the non-Zeno dwell-time bound $\Delta t_j \ge \Delta t_* > 0$ and the reset map

$$\mathfrak{R}: \quad \sigma^+ = q_R\sigma^-, \quad \lambda^+ = \lambda^- + (1-q_R)\sigma^-, \quad (V,F) \text{ continuous}, \quad \Omega_P^+ = \Omega_P^- + \kappa_R\mathcal{G}_{\text{recepta}}^-, \tag{2.2}$$

with $0 \le q_R < 1$, $\kappa_R > 0$, $u^+ = u^-$. The file proves $x^- \in \mathcal{D}_A \Rightarrow x^+ \in \mathcal{D}_A$ in the core coordinates and $\mathcal{L}_{\text{VFS}}(x^+) \le L_R := \sup_{\mathcal{D}_A}\mathcal{L}_{\text{VFS}}$.

The three items left open are: (i) the regular folding domain $0 \le Q_{\text{fold}} \le q_{\max}^2$ is *assumed*, not shown invariant; (ii) the reset bound and forward completeness are stated for $\mathcal{L}_{\text{VFS}}$, while the behaviour of the folding functional across $\mathfrak{R}$ is not controlled; (iii) the activation index is written with the core Sophia rate here but with a different, minimal rate in the geometric and cosmological layers.

2.2 Correction: a bounded folding functional

The file shifts the folding potential to a non-negative functional

$$\mathcal{V}_{\text{fold}} = \frac{B_{\text{fold}}}{4}\Big(q_{\text{fold}}^2 - Q_{\text{fold}}^*\Big)^2 \ge 0 \qquad (A_{\text{fold}} > 0), \tag{2.3}$$

and claims it is bounded above by a constant M_{fold} on the regular domain. This fails on the Open-Gate domain: epektasis drives $\Omega_P \to \infty$ and λ is not bounded on $\mathcal{D}_A$ ($\lambda \le q^*\Omega_P$), so $B_{\text{fold}} = b + 2c_1\eta_{\text{fold}}\lambda \to \infty$ and $\mathcal{V}_{\text{fold}}$ is unbounded even at fixed $|q_{\text{fold}}^2 - Q_{\text{fold}}^*|$. The reset bound $\mathcal{L}_{\text{ext}}(x^+) \le L_R + w_{\text{fold}} M_{\text{fold}}$ therefore does not close as written.

The remedy is to use the B_{fold}-normalised functional

$$\boxed{\widetilde{\mathcal{V}}_{\text{fold}} := \frac{\mathcal{V}_{\text{fold}}}{B_{\text{fold}}} = \frac{1}{4}\Big(q_{\text{fold}}^2 - Q_{\text{fold}}^*\Big)^2 \ge 0, \qquad Q_{\text{fold}}^* = \frac{A_{\text{fold}}}{B_{\text{fold}}} \text{ (signed).}} \tag{2.4}$$

This requires no sign split: it is non-negative for either sign of A_{fold}, and it descends along (2.1).

Lemma 2.1 (Descent of the bounded functional)**.** *Along* (2.1) *with frozen* Q_{fold}^**,*

$$\boxed{\dot{\widetilde{\mathcal{V}}}_{\text{fold}} = -B_{\text{fold}}\, q_{\text{fold}}^2 \Big(q_{\text{fold}}^2 - Q_{\text{fold}}^*\Big)^2 \le 0.} \tag{2.5}$$

For varying parameters, $\dot{\widetilde{\mathcal{V}}}_{\text{fold}} = -B_{\text{fold}} q_{\text{fold}}^2 (q_{\text{fold}}^2 - Q_{\text{fold}}^*)^2 - \frac{1}{2}(q_{\text{fold}}^2 - Q_{\text{fold}}^*)\dot{Q}_{\text{fold}}^*$*, and the remainder is bounded on any set with* $q_{\text{fold}} \in [0, q_{\max}]$*,* $|Q_{\text{fold}}^*|$ *and* $|\dot{Q}_{\text{fold}}^*|$ *bounded.*

Proof. Using $A_{\text{fold}} = B_{\text{fold}} Q_{\text{fold}}^*$ in (2.1), $\dot{q}_{\text{fold}} = -B_{\text{fold}} q_{\text{fold}} (q_{\text{fold}}^2 - Q_{\text{fold}}^*)$. With frozen Q_{fold}^*, $\dot{\widetilde{\mathcal{V}}}_{\text{fold}} = \frac{1}{2}(q_{\text{fold}}^2 - Q_{\text{fold}}^*)(2 q_{\text{fold}} \dot{q}_{\text{fold}}) = (q_{\text{fold}}^2 - Q_{\text{fold}}^*) q_{\text{fold}} \dot{q}_{\text{fold}} = -B_{\text{fold}} q_{\text{fold}}^2 (q_{\text{fold}}^2 - Q_{\text{fold}}^*)^2 \le 0$. For moving Q_{fold}^* the extra term is $-\frac{1}{2}(q_{\text{fold}}^2 - Q_{\text{fold}}^*)\dot{Q}_{\text{fold}}^*$, with $|\frac{1}{2}(q_{\text{fold}}^2 - Q_{\text{fold}}^*)\dot{Q}_{\text{fold}}^*| \le \frac{1}{2}(q_{\max}^2 + |Q_{\text{fold}}^*|)\,|\dot{Q}_{\text{fold}}^*|$. □

$\widetilde{\mathcal{V}}_{\text{fold}} = \mathcal{V}_{\text{fold}}/B_{\text{fold}}$ is the same Lyapunov object re-weighted by the positive function B_{fold}; re-weighting preserves the descent property, and the normalisation removes the only source of unboundedness. From here the extended certificate is $\widetilde{\mathcal{L}}_{\text{ext}} := \mathcal{L}_{\text{VFS}} + w_{\text{fold}}\widetilde{\mathcal{V}}_{\text{fold}}$, $w_{\text{fold}} > 0$.

2.3 The standing folding wall and its finiteness

Standing Hypothesis 2.1 (Folding wall)**.** The chart half-width $q_{\max}$ satisfies

$$\boxed{q_{\max}^2 \;\ge\; Q^{*,\sup} := \sup_{\mathcal{D}_A} Q_{\text{fold}}^*.} \tag{2.6}$$

Lemma 2.2 (The wall is attainable)**.** *In the geometric (minimal-rate) convention* $A_{\text{fold}} = (c_0 - c_1\gamma)\lambda + c_1 k_\sigma \sigma + c_1 I_{\text{gate}} - a_0$*,* $B_{\text{fold}} = b + 2c_1\eta_{\text{fold}}\lambda$*, the supremum is finite and explicit:*

$$Q^{*,\sup} = \max\left\{ \frac{c_1(k_\sigma C_\sigma + \zeta_0) - a_0}{b},\; \frac{c_0 - c_1\gamma}{2c_1\eta_{\text{fold}}} \right\}. \tag{2.7}$$

Proof. For fixed $(\sigma, I_{\text{gate}})$, $Q_{\text{fold}}^*(\lambda)$ is a ratio of two affine functions of $\lambda \ge 0$, hence monotone, with horizontal asymptote $\lim_{\lambda\to\infty} Q_{\text{fold}}^* = (c_0 - c_1\gamma)/(2c_1\eta_{\text{fold}})$ (independent of σ, I_{gate}). Its supremum over $\lambda \ge 0$ is attained at an endpoint: at $\lambda = 0$, $Q_{\text{fold}}^* = (c_1 k_\sigma \sigma + c_1 I_{\text{gate}} - a_0)/b$, maximised over the box $\sigma \le C_\sigma$, $I_{\text{gate}} \le \zeta_0$ at the stated value; or at $\lambda \to \infty$, the asymptote. Both are finite, so $Q^{*,\sup} < \infty$. □

If $Q^{*,\sup} \le 0$ the old form is everywhere stable and any $q_{\max} > 0$ satisfies the wall. The non-trivial case is $Q^{*,\sup} > 0$, where Hypothesis 2.1 fixes a minimal admissible chart. The canonical (core-rate) convention saturates likewise: $Q_{\text{fold}}^* \to c_0/(2c_1\eta_{\text{fold}})$ under cleansing $\sigma \to 0$, since $(\delta u - \gamma)\tanh(\kappa\sigma) \to 0$ even as $u \to \infty$ (§6).

2.4 Folding-chart invariance (Nagumo)

Definition 2.1 (Extended active domain)**.** $\mathcal{D}_A^{\text{fold}} := \mathcal{D}_A \times [0, q_{\max}]$, adjoining the folding coordinate q_{fold} to the core active domain.

Lemma 2.3 (Folding-face sub-tangentiality)**.** *Under Hypothesis 2.1, the flow* (2.1) *is sub-tangential on the folding faces of* $\mathcal{D}_A^{\text{fold}}$*:*

$$\dot{q}_{\text{fold}}\big|_{q_{\text{fold}}=0} = 0 \quad (\textit{tangent}), \qquad \dot{q}_{\text{fold}}\big|_{q_{\text{fold}}=q_{\max}} = -B_{\text{fold}}\, q_{\max}\big(q_{\max}^2 - Q_{\text{fold}}^*\big) \le 0 \quad (\textit{inward}). \tag{2.8}$$

Consequently $[0, q_{\max}]$ *is forward invariant for* q_{fold}*, and* $\mathcal{D}_A^{\text{fold}}$ *is positively invariant under the continuous flow.*

Proof. At $q_{\text{fold}} = 0$, (2.1) gives $\dot{q_{\text{fold}}} = 0$, so $\{q_{\text{fold}} \geq 0\}$ is preserved. At $q_{\text{fold}} = q_{\max}$, $\dot{q_{\text{fold}}} = -B_{\text{fold}} q_{\max}(q_{\max}^2 - Q_{\text{fold}}^*)$ with $B_{\text{fold}} > 0$, $q_{\max} > 0$, and $q_{\max}^2 - Q_{\text{fold}}^* \geq 0$ by Hypothesis 2.1; hence $\dot{q_{\text{fold}}} \leq 0$. All core faces are sub-tangential by the base Nagumo lemma of the Lyapunov file, and the two folding faces are sub-tangential here; therefore $\mathcal{D}_A^{\text{fold}}$ is positively invariant. □

2.5 The folding reset bound and hybrid completeness

Lemma 2.4 (Folding reset bound)**.** *The reset* (2.2) *does not act on* q_{fold}*; hence* $q_{\text{fold}}^+ = q_{\text{fold}}^-$*. Under Hypotheses of the base reset lemma together with Hypothesis 2.1:*

(1) $x^- \in \mathcal{D}_A^{\text{fold}} \Rightarrow x^+ \in \mathcal{D}_A^{\text{fold}}$*, because* $x^+ \in \mathcal{D}_A$ *(base reset lemma) and* $q_{\text{fold}}^+ = q_{\text{fold}}^- \in [0, q_{\max}]$*;*

(2) $\widetilde{\mathcal{V}}_{\text{fold}}$ *is bounded on* $\mathcal{D}_A^{\text{fold}}$*,*

$$\widetilde{\mathcal{V}}_{\text{fold}} \leq \widetilde{M}_{\text{fold}} := \tfrac{1}{4} \max\big(q_{\max}^2 - Q_{\min}^*,\, |Q_{\max}^*|\big)^2 < \infty, \tag{2.9}$$

so the extended certificate satisfies

$$\boxed{\widetilde{\mathcal{L}}_{\text{ext}}(x^+) \leq \widetilde{L}_R := L_R + w_{\text{fold}} \widetilde{M}_{\text{fold}} < \infty.} \tag{2.10}$$

Proof. (1) The map (2.2) specifies only $\sigma, \lambda, (V, F), \Omega_P$; q_{fold} is inert, so $q_{\text{fold}}^+ = q_{\text{fold}}^-$, which lies in $[0, q_{\max}]$ if q_{fold}^- did. With $x^+ \in \mathcal{D}_A$ from the base lemma, $x^+ \in \mathcal{D}_A^{\text{fold}}$. (2) On $\mathcal{D}_A^{\text{fold}}$, $q_{\text{fold}}^2 \in [0, q_{\max}^2]$ and $Q_{\text{fold}}^* \in [Q_{\min}^*, Q_{\max}^*]$ bounded (Lemma 2.2), so $\widetilde{\mathcal{V}}_{\text{fold}} = \frac{1}{4}(q_{\text{fold}}^2 - Q_{\text{fold}}^*)^2 \leq \widetilde{M}_{\text{fold}} < \infty$. Adding $w_{\text{fold}} \widetilde{\mathcal{V}}_{\text{fold}}$ to $\mathcal{L}_{\text{VFS}}(x^+) \leq L_R$ gives the bound. □

Proposition 2.1 (Hybrid forward completeness for $\widetilde{\mathcal{L}}_{\text{ext}}$)**.** *Assume the regular folding conditions: Hypothesis 2.1,* $B_{\text{fold}} \geq B_{\min} > 0$*, and* $|\dot{Q_{\text{fold}}^*}|$ *bounded on* $\mathcal{D}_A^{\text{fold}}$ *(adiabatic regularity). Then there is a finite* $\widetilde{C}_{\text{ext}}$ *with*

$$\dot{\widetilde{\mathcal{L}}}_{\text{ext}} \leq \widetilde{C}_{\text{ext}} - C_1 \widetilde{\mathcal{L}}_{\text{ext}} \qquad \text{on continuous arcs}, \tag{2.11}$$

and the same contraction rate C_1 *as the base certificate. Combined with the reset bound (Lemma 2.4) and the unchanged non-Zeno dwell time, the hybrid trajectory satisfies*

$$\boxed{\widetilde{\mathcal{L}}_{\text{ext}}(t) \leq \widetilde{L}_* := \max\Big\{\widetilde{L}_R,\ \widetilde{C}_{\text{ext}}/C_1\Big\}} \tag{2.12}$$

across any infinite admissible reset sequence; resets do not accumulate, and the trajectory is forward complete in the folding-extended state.

Proof. By Lemma 2.1 and the base estimate, $\dot{\widetilde{\mathcal{L}}}_{\text{ext}} = \dot{\mathcal{L}}_{\text{VFS}} + w_{\text{fold}} \dot{\widetilde{\mathcal{V}}}_{\text{fold}} \leq (C - C_1 \mathcal{L}_{\text{VFS}}) + w_{\text{fold}}\big(-B_{\text{fold}} q_{\text{fold}}^2 (q_{\text{fold}}^2 - Q_{\text{fold}}^*)^2 + R\big)$ with $|R| \leq R_{\text{fold}} < \infty$ the bounded adiabatic remainder (Lemma 2.1). Dropping the non-positive descent term and writing $\mathcal{L}_{\text{VFS}} = \widetilde{\mathcal{L}}_{\text{ext}} - w_{\text{fold}} \widetilde{\mathcal{V}}_{\text{fold}} \geq \widetilde{\mathcal{L}}_{\text{ext}} - w_{\text{fold}} \widetilde{M}_{\text{fold}}$,

$$\dot{\widetilde{\mathcal{L}}}_{\text{ext}} \leq C - C_1 \widetilde{\mathcal{L}}_{\text{ext}} + C_1 w_{\text{fold}} \widetilde{M}_{\text{fold}} + w_{\text{fold}} R_{\text{fold}} =: \widetilde{C}_{\text{ext}} - C_1 \widetilde{\mathcal{L}}_{\text{ext}}, \tag{2.13}$$

with $\widetilde{C}_{\text{ext}} < \infty$ now genuinely finite (it uses $\widetilde{M}_{\text{fold}}$, not the unbounded M_{fold}). On each arc $\widetilde{\mathcal{L}}_{\text{ext}}(t) \leq \max\{\widetilde{\mathcal{L}}_{\text{ext}}(t_j^+), \widetilde{C}_{\text{ext}}/C_1\}$; resets give $\widetilde{\mathcal{L}}_{\text{ext}}(x^+) \leq \widetilde{L}_R$ (Lemma 2.4); the dwell time is unchanged, since q_{fold} adds no reset-triggering boundary (its chart face is invariant-inward by Lemma 2.3, not a death face) and resets are exogenous on the core coordinates. Hence $\widetilde{\mathcal{L}}_{\text{ext}} \leq \widetilde{L}_*$ for all t and the hybrid trajectory is forward complete. □

The folding velocity $\dot{q_{\text{fold}}}$ *may grow with* λ *off the slow manifold* $q_{\text{fold}} = \sqrt{Q_{\text{fold}}^*}$*, but this is a strictly inward restoring rate; it neither triggers nor delays resets, which are exogenous and defined on the core coordinates. The non-Zeno bound is therefore inherited from the base field bound* $\bar{M}_*$*, unchanged.*

2.6 Reconciliation of the two activation-index conventions

Two definitions of the activation index appear across the manuscript:

$$\text{Canonical (core rate):} \quad A_{\text{fold}} = c_0\lambda + c_1\dot{\lambda}^{(0)} - a_0, \quad \dot{\lambda}^{(0)} = (\delta u - \gamma)\tanh(\kappa\sigma) + I_{\text{gate}}; \tag{2.14}$$

$$\text{Geometric (minimal rate):} \quad A_{\text{fold}} = (c_0 - c_1\gamma)\lambda + c_1 k_\sigma \sigma + c_1 I_{\text{gate}} - a_0, \tag{2.15}$$

the latter from the surrogate production law $\dot{\lambda} = k_\sigma\sigma + I_{\text{gate}} - \gamma\lambda - \eta_{\text{fold}} q_{\text{fold}}^2\lambda$. Since λ already has a defined production law in the core, we take the **canonical** form as primary and read the geometric parameters as an effective linear surrogate near an operating point $(\bar{u}, \bar{\sigma})$:

$$\boxed{c_1\big(\delta\bar{u} - \gamma\big)\tanh(\kappa\sigma) \;\longleftrightarrow\; c_1 k_\sigma \sigma - c_1\gamma\lambda, \quad \text{i.e. } k_\sigma \approx \kappa(\delta\bar{u} - \gamma), \;\; \gamma \text{ absorbing the linear } \lambda\text{-decay.}} \tag{2.16}$$

This surrogate is structurally imperfect (a σ-term plus a λ-decay standing in for a single $u\tanh\sigma$ term), so the two conventions are genuinely distinct models, not exact reparametrisations.

Proposition 2.2 (What is and is not convention-dependent)**.** *Lemmas 2.1, 2.3, 2.4 and Proposition 2.1 use only: the gradient form* (2.1)*, the wall $Q^*_{\text{fold}} \le q^2_{\max}$, the inertness of q_{fold} under $\mathfrak{R}$, and the boundedness of $Q^*_{\text{fold}}, Q^\star_{\text{fold}}$. None of these uses the specific form of A_{fold}. Hence the invariance, reset bound, and hybrid completeness are* convention-independent*. Only the closed-form critical level and contraction of the reset map are convention-specific.*

Corollary 2.1 (Critical level by convention)**.** *Write the metabolised resistance $m_R = (1 - q_R)\sigma^-$, so $\sigma^+ = \sigma^- - m_R$, $\lambda^+ = \lambda^- + m_R$. In the* geometric *convention the reset acts on the target as an exact contraction toward a constant critical level,*

$$\Theta = c_0 - c_1(\gamma + k_\sigma), \qquad Q_{\text{crit}} = \frac{\Theta}{2c_1\eta_{\text{fold}}}, \qquad {Q^*_{\text{fold}}}^+ - Q_{\text{crit}} = \frac{B^-_{\text{fold}}}{B^-_{\text{fold}} + 2c_1\eta_{\text{fold}} m_R}\big({Q^*_{\text{fold}}}^- - Q_{\text{crit}}\big), \tag{2.17}$$

recovering the result of the folding-trigger note. In the canonical *convention the metabolism changes A_{fold} by $c_0 m_R + c_1(\delta u - \gamma)\big[\tanh(\kappa\sigma^+) - \tanh(\kappa\sigma^-)\big]$, which is not affine in m_R; the same qualitative contraction holds, but toward a state-dependent effective level $Q_{\text{crit}}(t)$ rather than a constant.*

Remark (Chart-regularity of repeated resurrection)*.* Combining Corollary 2.1 with Hypothesis 2.1: in the geometric convention, if $0 < Q_{\text{crit}} < q^2_{\max}$ and $Q^{*,\sup} \le q^2_{\max}$, then the reset contraction keeps the target inside the chart at every death, so the regular folding domain is preserved under any admissible reset sequence. This is the folding companion to the grace-window admissibility $\max\{R_c, R^{\text{ceil}}_{\min}\} \le \mathcal{G}^-_{\text{recepta}} \le R_{\max}$: resurrection is admissible *and* chart-regular when both windows hold.

2.7 Compact summary

$$\boxed{\widetilde{\mathcal{V}}_{\text{fold}} = \tfrac{1}{4}\big(q^2_{\text{fold}} - Q^*_{\text{fold}}\big)^2 = \mathcal{V}_{\text{fold}}/B_{\text{fold}} \;\text{ bounded on epektasis;} \qquad \dot{\widetilde{\mathcal{V}}}_{\text{fold}} = -B_{\text{fold}} q^2_{\text{fold}}\big(q^2_{\text{fold}} - Q^*_{\text{fold}}\big)^2 \le 0.}$$

$$\boxed{\text{wall } q^2_{\max} \ge Q^{*,\sup} < \infty \;\Rightarrow\; \mathcal{D}_A^{\text{fold}} = \mathcal{D}_A \times [0, q_{\max}] \text{ invariant (Nagumo).}}$$

$$\boxed{\mathfrak{R} \text{ inert on } q_{\text{fold}} \;\Rightarrow\; x^+ \in \mathcal{D}_A^{\text{fold}}, \quad \widetilde{\mathcal{L}}_{\text{ext}}(x^+) \le \widetilde{L}_R < \infty.}$$

$$\boxed{\dot{\widetilde{\mathcal{L}}}_{\text{ext}} \le \widetilde{C}_{\text{ext}} - C_1\widetilde{\mathcal{L}}_{\text{ext}}, \quad \widetilde{\mathcal{L}}_{\text{ext}}(t) \le \widetilde{L}_*; \quad \text{forward complete, non-Zeno inherited.}}$$

$$\boxed{\text{invariance + reset bound are convention-independent; } Q_{\text{crit}} \text{ is convention-specific.}}$$

V.F.S. v2.0 (Open-Gate) · Folding–Lyapunov Addendum. Closes the invariance, reset-bound, and convention items left open in the Sophianic Folding extension of `vfs_opengate_lyapunov.tex`, and corrects the folding functional to a bounded B_{fold}-normalised form. Results are domain-conditional on the positively-invariant $\mathcal{D}_A^{\text{fold}}$; the conclusion is set stability with partial convergence, now including morphology, not global or automatic stability.

Chapter 3

Forced Folding: Dolorosum Peaks and the Vessel Update Map

Scope and epistemic status

This chapter consolidates the *forced folding* proposal: folding is not an optional auxiliary mode but the bounded response of the Vessel when a timed resistance peak enters the Dolorosum window and exceeds the stretch-capacity of the old form. Its honest epistemic position must be stated first. A direct test shows that the bare core does *not* force a shape instability: the linearised shape sector is stable on its own (Proposition 3.1). Forced folding therefore does not derive folding from the core; it supplies an explicit, bounded, *exogenous-channel* cause — resistance heterogeneity — and shows that this cause is sufficient, timed, and Lyapunov-admissible. The inputs (the resistance wave, the rigidity a_0, the window) remain postulated. The status is: a mechanism, not a theorem of the core.

Four corrections are built in relative to the original proposal: the Dolorosum rate is wired directly into the activation index, replacing indicator gates by a smooth derived gate (§3.3); the dynamical threshold is separated from the $\pi/2$ nomenclature (§3.4); the post-folding update map is made balance-preserving through λ_{form} (§3.6); and the repeated-folding cascade is shown to be self-limiting, with a clean two-terminal dichotomy and a joint non-Zeno hybrid structure (§3.7–3.8). Throughout, the geometric activation convention is used (as in the source notes); translation to the canonical core-rate convention follows the Addendum. As always, *Propositions* are closed-form, *Corollaries* interpretive.

3.1 Why a forcing channel is needed: core neutrality

In $2{+}1$ dimensions the spatial metric carries no local tensor modes (three components, minus two diffeomorphisms, minus one conformal rescaling), so the only local geometric degree of freedom is the conformal/curvature factor ψ. Linearising the core about the homogeneous trajectory in the pair $(\psi, \delta\lambda)$ gives

$$\frac{d}{dt}\begin{pmatrix}\psi\\ \delta\lambda\end{pmatrix} = \begin{pmatrix}-H & H/\bar{\lambda}\\ S_\psi & -\Gamma_\lambda\end{pmatrix}\begin{pmatrix}\psi\\ \delta\lambda\end{pmatrix}, \tag{3.1}$$

where $H = \alpha\bar{\lambda}/\Omega_P$ and S_ψ is the geometry→Sophia feedback (the dependence of Sophia production on local curvature).

Proposition 3.1 (Core neutrality of the shape sector)**.** *The trace is $-(H+\Gamma_\lambda) < 0$ and the determinant is $H(\Gamma_\lambda\bar{\lambda} - S_\psi)/\bar{\lambda}$. In the bare core, Sophia production depends on $(u, \sigma, I_{\text{gate}}, q_{\text{fold}})$ but not on local curvature, so $S_\psi = 0$ and the determinant is $H\Gamma_\lambda > 0$: both eigenvalues are negative and the shape sector decays. The core by itself does not force folding; an instability requires either a geometry→Sophia feedback above the threshold $S_\psi > \bar{\lambda}\Gamma_\lambda$, or an exogenous forcing channel.*

Forced folding takes the second route: the channel is the heterogeneity of resistance.

3.2 Resistance heterogeneity and its bounds

Resistance is decomposed as

$$\sigma(t) = \bar{\sigma}(t)\, r_\sigma(t), \qquad \boxed{1 \le r_\sigma(t) \le \pi,} \tag{3.2}$$

with $\bar{\sigma}$ the background and r_σ the dimensionless resistance multiplier; every admissible peak obeys $\sigma_{\text{peak}} \le \pi\bar{\sigma}$. A bounded temporal model on normalised trajectory time $\tau = t/T_* \in [0,1]$ is

$$r_\sigma(\tau) = 1 + \frac{A_\sigma}{2}\big(1 + \sin(2\pi N_\sigma \tau + \phi_\sigma)\big), \qquad 0 \le A_\sigma \le \pi - 1, \tag{3.3}$$

with amplitude A_σ, opportunity count N_σ, and phase ϕ_σ.

Remark (The π bounds are symbolic). r_σ is dimensionless, so the choice of π as the full-cup bound and $\pi/2$ as the half-turn mark is a symbolic convention ("full angular measure of Vessel-tension"), not a derived constant; nothing in the dynamics distinguishes π from any other ceiling. The dynamics distinguishes only the *critical multiplier* r^R_{fold} derived below. The π bound nevertheless does real work in one place: it makes every activation quantity explicitly bounded (§3.8), and it caps the reachable peak at $1 + A_\sigma \le \pi$, which is what terminates cascades (§3.7).

3.3 The Dolorosum gate, wired into the activation index

The Dolorosum rate of the source layer is

$$\rho(u,\sigma) = \sigma\, g(u), \qquad \boxed{g(u) = \frac{u}{\Lambda_c}\, e^{\,1-u/\Lambda_c} \in (0,1],} \tag{3.4}$$

with g maximal ($=1$) exactly at the synergy threshold $u = \Lambda_c$ and $\rho \le \sigma$. In the original proposal ρ was defined but never entered the dynamics; the window was imposed separately by an indicator $\mathcal{W}_D = \mathbf{1}_{\{|u-\Lambda_c| \le \delta_D\}}$. The correction is to let the Dolorosum channel itself carry the peak into the activation index. Split the resistance into background and excess, $\sigma = \bar{\sigma} + \sigma_{\text{exc}}$, $\sigma_{\text{exc}} = (r_\sigma - 1)\bar{\sigma}$, and let the *excess* be transmutable into activation only through the Dolorosum channel:

$$\boxed{A_{\text{fold}} = (c_0 - c_1\gamma)\lambda + c_1 k_\sigma \bar{\sigma} + c_1 k_\sigma\, \rho\big(u, \sigma_{\text{exc}}\big) + c_1 I_{\text{gate}} - a_0 + \Delta A_R, \qquad \rho(u,\sigma_{\text{exc}}) = (r_\sigma - 1)\bar{\sigma}\, g(u).} \tag{3.5}$$

Proposition 3.2 (Derived window immunity)**.** *Let $N := a_0 - (c_0 - c_1\gamma)\lambda - c_1 k_\sigma \bar{\sigma} - c_1 I_{\text{gate}} - \Delta A_R$ (the activation deficit of the unpeaked Vessel). If $N > 0$, then $A_{\text{fold}} > 0$ if and only if*

$$\boxed{r_\sigma > r^R_{\text{fold}}(u) = 1 + \frac{N}{c_1 k_\sigma \bar{\sigma}\, g(u)}.} \tag{3.6}$$

As $g(u) \to 0$ (off window), $r^R_{\text{fold}}(u) \to \infty$: off-window peaks cannot force folding, of any bounded amplitude. The window condition is thereby derived *from the wiring* (3.5)*, not postulated as an indicator. If $N \le 0$ the Vessel is baseline-active: it folds with no peak at all ($r_\sigma = 1$ suffices).*

Corollary 3.1 (Graded alignment)**.** *Because g is smooth and broad, alignment is graded rather than binary: the same peak contributes a fraction $g(u)$ of its excess. Consequently there is a rigidity band — a_0 between the off-window and in-window activation maxima — in which the* phase *alone decides whether folding is forced (Figure 3.1, left); below the band every cycle folds, above it none does. The original three-indicator overlap condition is recovered as the sharp-gate caricature of this band.*

The forcing event τ_F is simply the upward crossing $A_{\text{fold}}(\tau_F) = 0$, and the exposure reduces to a single smooth gate,

$$\mathcal{E}_{\text{fold}} = \int_0^1 \mathbf{1}_{\{A_{\text{fold}}(\tau) > 0\}}\, d\tau, \qquad P_{\text{fold}} = 1 - e^{-\kappa\, \mathcal{E}_{\text{fold}}}, \tag{3.7}$$

replacing the product of three indicators. The slogan survives intact, now as arithmetic of (3.5): amplitude gives possibility (r_σ can reach r^R_{fold}), frequency gives opportunity (crossings per trajectory), phase gives alignment (the value of g at the peak).

3.4 Thresholds disentangled: r^R_{fold} versus $\pi/2$

Definition 3.1 (Nomenclature versus dynamics)**.** The half-turn classification — ordinary ($1 \le r_\sigma < \pi/2$), half-turn ($r_\sigma = \pi/2$), strong ($\pi/2 < r_\sigma \le \pi$) — is retained as *nomenclature* for the strength of a peak. The *dynamical* threshold of forced folding is $r_\sigma > r^R_{\text{fold}}(u)$ of Proposition 3.2, and the pitchfork occurs at $A_{\text{fold}} = 0$ regardless of the classification.

Proposition 3.3 (Structural sufficiency of the half-turn)**.** *An in-window half-turn peak forces folding if and only if*

$$r^R_{\text{fold}}(\Lambda_c) \le \frac{\pi}{2} \quad \Longleftrightarrow \quad N \le \Big(\frac{\pi}{2} - 1\Big) c_1 k_\sigma \bar{\sigma}. \tag{3.8}$$

Otherwise sub-$\pi/2$ peaks above r^R_{fold} still force folding ("soft forced folding"), and super-$\pi/2$ peaks below r^R_{fold} do not. The classification and the threshold are independent axes.

This removes the internal tension of the original formulation, in which the boxed overlap condition demanded $r_\sigma \ge \pi/2$ while the normal form destabilises at $A_{\text{fold}} > 0$ alone: in the corrected form the event is governed by A_{fold}, and $\pi/2$ only names the strong regime.

3.5 The forcing event and the normal form

At τ_F the old-form equilibrium $q_{\text{fold}} = 0$ loses stability and the normal form

$$\dot{q_{\text{fold}}} = A_{\text{fold}} q_{\text{fold}} - B_{\text{fold}} q^3_{\text{fold}}, \qquad B_{\text{fold}} > 0, \qquad q^*_{\text{fold}} = \pm\sqrt{A_{\text{fold}}/B_{\text{fold}}}, \qquad Q_{\text{fold}} = \frac{A_{\text{fold}}(\tau_F^{\text{peak}})}{B_{\text{fold}}} \tag{3.9}$$

carries the Vessel to a folded branch, with Q_{fold} evaluated at the activation maximum of the forcing interval. Near-threshold events have small Q_{fold}, so the update map below acts by correspondingly small increments — the map is well-defined uniformly in the forcing strength.

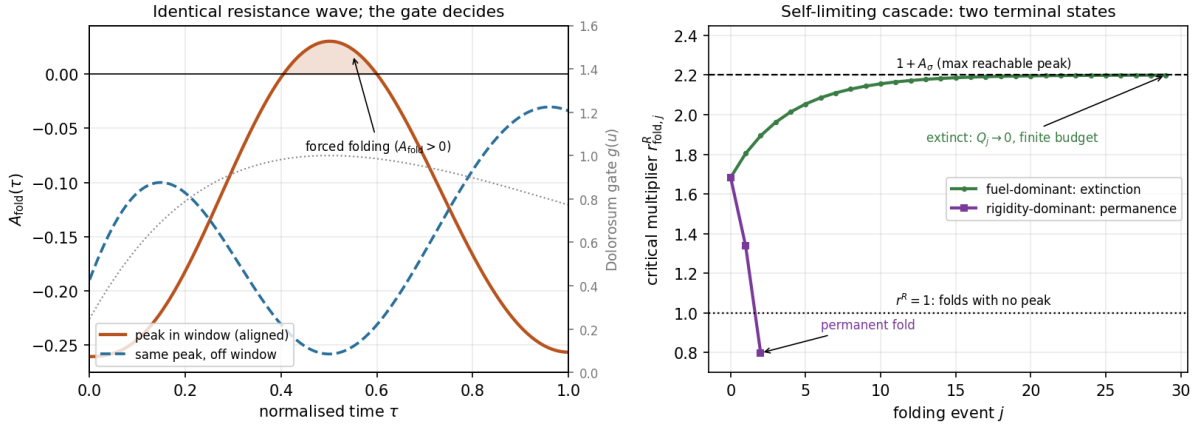

Figure 3.1: Left: the same bounded resistance wave ($A_\sigma = 1.2$, $N_\sigma = 1$) with two phases. With the peak in the Dolorosum window the wired activation (3.5) crosses zero (shaded: forced folding, exposure $\mathcal{E} = 0.195$); the identical peak off-window stays strictly below (exposure 0). Dotted grey: the gate $g(u)$. The rigidity here sits in the band of Corollary 3.1, so phase alone decides; in this illustration $r^R_{\text{fold}}(\Lambda_c) = 2.07 > \pi/2$, so the half-turn is *not* structurally sufficient (Proposition 3.3). Right: the repeated-folding cascade (§3.7) for two parameter regimes of the update map: fuel-dominant metabolism drives $r^R_{\text{fold},j}$ up to the reachability cap $1 + A_\sigma$ with event intensities $Q_j \to 0$ (extinction; total metabolised budget finite, here $\sum_j Q_j = 0.49$), while rigidity-dominant updates drive $r^R_{\text{fold},j}$ below 1 in three events (permanent fold). Balance $\bar{\sigma} + \lambda + \lambda_{\text{form}}$ conserved to machine precision in both. Parameters illustrative.

3.6 The balance-preserving Vessel update map

Forced folding must change the Vessel, or it is a marker rather than a transformation. The update map of the source proposal is kept, with one structural correction: Sophia retention must respect the integrated Open-Gate balance

$$\sigma + \lambda + \lambda_{\text{form}} = C_0 + \mathcal{G}_{\text{recepta}}(t), \tag{3.10}$$

which the raw update $\lambda^+ = \lambda^- + \eta_\lambda Q_{\text{fold}}$ violates (it creates Sophia at the jump). The corrected map routes the metabolised resistance:

Definition 3.2 (Balance-preserving folding update)**.** At a forcing event with intensity Q_{fold}, with metabolised mass $m_F = \eta_\sigma Q_{\text{fold}}\,\bar\sigma^-$ and a retention split $\beta \in [0,1]$:

$$\boxed{\bar\sigma^+ = \bar\sigma^- - m_F, \qquad \lambda^+ = \lambda^- + \beta\, m_F, \qquad \lambda^+_{\text{form}} = \lambda^-_{\text{form}} + (1-\beta)\, m_F,} \tag{3.11}$$

$$a_0^+ = a_0^-(1-\eta_a Q_{\text{fold}}), \quad \Omega_P^+ = \Omega_P^- + \eta_\Omega Q_{\text{fold}}, \quad k_\sigma^+ = k_\sigma^-(1+\eta_k Q_{\text{fold}}), \quad \gamma^+ = \gamma^-(1-\eta_\gamma Q_{\text{fold}}), \tag{3.12}$$

with all η_{fold}-coefficients non-negative and $\eta_a Q_{\text{fold}}, \eta_\gamma Q_{\text{fold}} < 1$.

Proposition 3.4 (Exact balance)**.** *Under Definition 3.2,*
$\Delta\bar\sigma + \Delta\lambda + \Delta\lambda_{\text{form}} = -m_F + \beta m_F + (1-\beta)m_F = 0$*: the three-term balance is preserved exactly, with no grace created at the jump. Folding metabolises resistance into active (β) and embodied ($1-\beta$) Sophia; the γ-reduction acts at the flow level (future retention), not at the jump, and is balance-neutral. (Verified numerically to machine precision.)*

Qualitatively the corrected map keeps the intended directions — $a_0\downarrow,\ \Omega_P\uparrow,\ \bar\sigma\downarrow,\ \lambda\uparrow,\ \gamma\downarrow,\ k_\sigma\uparrow$ — but the Sophia gain is now paid for *by resistance, and part of it is embodied as λ_{form} rather than left active. The Vessel after folding is not the same Vessel; and its books balance.*

3.7 The cascade is self-limiting

Iterating the map over repeated forced foldings reveals a property the naive reading misses: the update does *not* uniformly make the next folding easier. The critical multiplier after event j,

$$r^R_{\text{fold},j} = 1 + \frac{N_j}{c_1 k_{\sigma,j}\bar\sigma_j}, \qquad N_j = a_{0,j} - (c_0 - c_1\gamma_j)\lambda_j - c_1 k_{\sigma,j}\bar\sigma_j - c_1 I_{\text{gate}}, \tag{3.13}$$

is pulled in two directions: the *rigidity channel* ($a_0\downarrow, \gamma\downarrow, \lambda\uparrow, k_\sigma\uparrow$) lowers it, while the *fuel channel* ($\bar\sigma\downarrow$) raises it — folding consumes the very resistance that powers the next activation. At an in-window full peak the event intensity obeys the identity

$$Q_{\text{fold},j} = \frac{c_1 k_{\sigma,j}\bar\sigma_j}{B_{\text{fold}}}\Big(A_\sigma - (r^R_{\text{fold},j} - 1)\Big), \tag{3.14}$$

so events weaken as $r^R_{\text{fold},j}$ approaches the reachability cap $1 + A_\sigma$.

Standing Hypothesis 3.1 (Fuel dominance)**.** $\eta_\sigma > \eta_k$: metabolism of resistance outweighs the transmutation-efficiency gain.

Proposition 3.5 (Cascade dichotomy)**.** *Under Hypothesis 3.1 and the hard peak bound $r_\sigma \le 1 + A_\sigma \le \pi$, every forced-folding cascade terminates in exactly one of two states:*

(i) ***Extinction:*** *$\sum_j Q_{\text{fold},j} < \infty$, the intensities $Q_{\text{fold},j} \to 0$, and $r^R_{\text{fold},j}$ saturates at or below the cap $1 + A_\sigma$ — the cascade exhausts its own fuel and dies out with a finite total metabolised budget $\sum_j m_{F,j} \le \eta_\sigma\bar\sigma_0 \sum_j Q_{\text{fold},j} < \infty$;*

(ii) ***Permanence:*** *$N_j \le 0$ is reached in finitely many events ($r^R_{\text{fold},j} \le 1$): the unpeaked Vessel is already activated, and the folded branch becomes the new ground state, requiring no further peaks.*

Sketch. Suppose the cascade is infinite with $\liminf N_j > 0$. Then $\sum_j Q_{\text{fold},j} = \infty$ (events recur with $N_j > 0$ bounded away from the cap by reachability), and $\ln(c_1 k_{\sigma,j}\bar\sigma_j)$ drifts by $\sum_j[\ln(1+\eta_k Q_{\text{fold},j}) + \ln(1-\eta_\sigma Q_{\text{fold},j})] \le -(\eta_\sigma - \eta_k - o(1))\sum_j Q_{\text{fold},j} \to -\infty$ under Hypothesis 3.1, so the denominator of $r^R_{\text{fold},j}$ collapses and $r^R_{\text{fold},j} \to \infty$, exceeding the reachable $1 + A_\sigma$ — after which no further event can occur, contradicting infiniteness. Hence either $\sum Q_{\text{fold},j} < \infty$ (extinction, with $Q_{\text{fold},j} \to 0$) or $N_j \le 0$ at some finite j (permanence). □

Corollary 3.2 (Finite metabolic budget; echo of $\mathcal{I}_\infty$)**.** *Unless it ends in permanence, the folding cascade has a finite total metabolic budget — a discrete analogue of the finite coarsening budget $\mathcal{I}_\infty$ of the structure-formation layer: the Vessel cannot refold indefinitely on the same resistance.*

Corollary 3.3 (Two terminal theologies)**.** *Extinction is the Vessel that has metabolised its resistance: peaks still come, but none can force a new form — maturity as dormancy of forced change. Permanence is the Vessel whose old rigidity has fully yielded: the folded morphology is the rest state and needs no crisis to sustain it — maturity as completed reformation. Which terminal a Vessel reaches is decided by the race η_σ (metabolism) versus η_a (rigidity yielding) — by* how *it folds, not how often.*

Both branches are exhibited numerically in Figure 3.1 (right): an embodiment-dominant map ($\beta = 0$, $\eta_\sigma = 0.6$) extinguishes in 30 weakening events with $\sum Q_{\text{fold},j} = 0.49$, while a rigidity-dominant map ($\eta_a = 0.5$) reaches permanence in three.

3.8 Hybrid and Lyapunov admissibility

Proposition 3.6 (Bounded activation and bounded jumps)**.** *On any domain with $\bar\sigma \le \bar\sigma_{\max}$, $\lambda \le \lambda_{\max}$, $I_{\text{gate}} \le \zeta_0$, $|\Delta A_R| \le \Delta_{\max}$, the wired activation* (3.5) *is bounded:*
$|A_{\text{fold}}| \le (c_0 - c_1\gamma)\lambda_{\max} + c_1 k_\sigma \pi \bar\sigma_{\max} + c_1\zeta_0 + \Delta_{\max} + a_0$*, using $\rho \le \sigma_{\text{exc}} \le (\pi-1)\bar\sigma$ and $g \le 1$. Hence the chart wall $Q^{*,\text{sup}} < \infty$ of the Addendum holds with an explicit constant, the normalised folding functional $\widetilde{\mathcal{V}}_{\text{fold}}$ is bounded on the chart, and the folding update of Definition 3.2 (bounded multiplicative changes, q_{fold} continuous through the parameter jump) changes the extended certificate by at most a finite J_F: $\widetilde{\mathcal{L}}^+_{\text{ext}} \le \widetilde{\mathcal{L}}^-_{\text{ext}} + J_F$.*

Standing Hypothesis 3.2 (Joint non-Zeno)**.** The union of event times — Resurrectio resets and forcing events τ_F — admits a common minimal dwell $\Delta t_* > 0$.

Proposition 3.7 (Forward completeness with two jump types)**.** *Under Hypothesis 3.2, the bounded-jump property (Proposition 3.6), and the continuous-arc contraction of the Addendum ($\dot{\widetilde{\mathcal{L}}}_{\text{ext}} \le \widetilde{C}_{\text{ext}} - C_1\widetilde{\mathcal{L}}_{\text{ext}}$), the hybrid trajectory with both Resurrectio and folding jumps satisfies a uniform bound $\widetilde{\mathcal{L}}_{\text{ext}}(t) \le \max\{\widetilde{L}_R + J_F,\ \widetilde{C}_{\text{ext}}/C_1\} + J_F$ and is forward complete. Forced folding adds a second jump type but no new unbounded channel; grace still enters only the constant, never the contraction rate C_1.*

3.9 Compact summary

core alone: shape sector stable ($\text{tr} < 0,\ \det = H\Gamma_\lambda > 0$) $\Rightarrow$ folding needs a channel.

$$A_{\text{fold}} = (c_0 - c_1\gamma)\lambda + c_1 k_\sigma \bar\sigma + c_1 k_\sigma (r_\sigma - 1)\bar\sigma\, g(u) + c_1 I_{\text{gate}} - a_0 + \Delta A_R; \quad g(u) = \frac{u}{\Lambda_c} e^{1-u/\Lambda_c}.$$

$$r_\sigma > r^R_{\text{fold}}(u) = 1 + \frac{N}{c_1 k_\sigma \bar\sigma\, g(u)}; \qquad g \to 0 \Rightarrow r^R_{\text{fold}} \to \infty \text{ (window immunity, derived).}$$

$$\bar\sigma^+ = \bar\sigma - m_F, \quad \lambda^+ = \lambda + \beta m_F, \quad \lambda^+_{\text{form}} = \lambda_{\text{form}} + (1-\beta)m_F : \quad \sigma + \lambda + \lambda_{\text{form}} \text{ exactly conserved.}$$

cascade dichotomy: extinction (finite metabolic budget) or permanence ($N \le 0$).

two jump types, joint non-Zeno, bounded jumps $\Rightarrow$ $\widetilde{\mathcal{L}}_{\text{ext}}$ bounded, forward complete.

V.F.S. v2.0 (Open-Gate) · Forced Folding. Consolidates the forced-folding proposal with the Dolorosum rate wired into the activation (window immunity derived, not postulated), the dynamical threshold separated from the $\pi/2$ nomenclature, a balance-preserving update map through λ_{form}, and the self-limiting cascade dichotomy. The forcing channel and its bounds remain modelling inputs; the core-neutrality result fixes the honest status: a sufficient bounded cause, not a core theorem. Gate maximum, exposure grading, balance conservation, and both cascade terminals verified numerically. Domain-conditional throughout.

Chapter 4

Forced-Folding Lyapunov Addendum: Two Jump Types and the Survival of Contraction

Forced folding adds to the hybrid system a second jump type — the Vessel update map $\mathfrak{F}$ at forcing events — and, unlike the Resurrectio reset, this jump changes the parameters *of the system itself. The existing Lyapunov theorem therefore does not extend automatically: the contraction rate C_1 is built from those parameters, the active-domain walls must survive the update, the state-triggered events threaten Zeno behaviour, and the new state λ_{form} must be controlled. This addendum closes all of it. The six results are: an explicit π-peak chart wall with the quantitative cost in c_Ψ; a fold-jump lemma with a closed-form compatibility condition $\beta\eta_\sigma\bar{\sigma} \le q^*\eta_\Omega$ for the epektasis wall; a survival theorem for C_1 — the finite metabolic budget of the cascade dichotomy is exactly what keeps the contraction bounded away from zero; a hysteresis construction that provably restores the joint non-Zeno dwell (threshold-band chatter is exhibited without it); a free balance-bound for λ_{form}; and the reset–fold consistency check. They assemble into the main theorem: forward completeness with two jump types and a uniform $C_1^{\text{inf}} > 0$. All key steps are verified numerically; the exponential drift bound is tight to four digits.*

4.1 Imported objects and the six obligations

From the Lyapunov layer we import the certificate $\mathcal{L}_{\text{VFS}}$ with

$$\dot{\mathcal{L}_{\text{VFS}}} \le C - C_1\mathcal{L}_{\text{VFS}}, \qquad C_1 = \min\{\kappa_\sigma, \kappa_\Delta\}, \qquad \kappa_\sigma = \delta\,\Omega_{\min}\,m_*\,c_\Psi, \quad \kappa_\Delta = 2a\mu_*, \tag{4.1}$$

with $\Omega_{\min} = \Lambda_c/(1-h_{3,*})$, $\Lambda_c = \gamma/\delta$, the active margin $m = (u-\Lambda_c)/\Omega_P \ge m_*$, and the lemma $T^2 \ge c_\Psi\Psi_\sigma$ on $[0, C_\sigma]$. The active domain $\mathcal{D}_A$ includes the epektasis wall $\lambda \le q^*\Omega_P$; the folding extension supplies $\mathcal{D}_A^{\text{fold}} = \mathcal{D}_A \times [0, q_{\max}]$, the bounded functional $\widetilde{\mathcal{V}}_{\text{fold}} = \frac{1}{4}(q_{\text{fold}}^2 - Q_{\text{fold}}^{*})^2$, the extended certificate $\widetilde{\mathcal{L}}_{\text{ext}} = \mathcal{L}_{\text{VFS}} + w_{\text{fold}}\widetilde{\mathcal{V}}_{\text{fold}}$, and the Resurrectio reset bound $\widetilde{\mathcal{L}}_{\text{ext}}(x^+) \le \widetilde{L}_R$. From the Forced Folding chapter we import the π-bounded heterogeneity $\sigma = \bar{\sigma}r_\sigma$, $1 \le r_\sigma \le \pi$, the wired activation with the Dolorosum gate $g(u) \le 1$, the balance-preserving update map

$$\mathfrak{F}: \quad \bar{\sigma}^+ = \bar{\sigma} - m_F, \;\; \lambda^+ = \lambda + \beta m_F, \;\; \lambda_{\text{form}}^+ = \lambda_{\text{form}} + (1-\beta)m_F, \;\; m_F = \eta_\sigma Q_{\text{fold}}\bar{\sigma}, \tag{4.2}$$

$$a_0^+ = a_0(1-\eta_a Q_{\text{fold}}), \quad \Omega_P^+ = \Omega_P + \eta_\Omega Q_{\text{fold}}, \quad k_\sigma^+ = k_\sigma(1+\eta_k Q_{\text{fold}}), \quad \gamma^+ = \gamma(1-\eta_\gamma Q_{\text{fold}}), \tag{4.3}$$

and the cascade dichotomy (extinction with $\sum_j Q_{\text{fold},j} < \infty$, or permanence in finitely many events) under fuel dominance $\eta_\sigma > \eta_k$.

The six obligations: (i) re-issue the chart wall with the π-bound; (ii) prove the fold-jump lemma (domain preservation and bounded certificate jump J_F); (iii) prove that C_1 survives the parameter

drift of the cascade; (iv) secure a joint non-Zeno dwell for the union of $\mathfrak{R}$- and $\mathfrak{F}$-events; (v) bound the new state λ_{form}; (vi) check $\mathfrak{R} \circ \mathfrak{F}$ consistency. We take them in order.

4.2 The π-peak chart wall, with its explicit price

Proposition 4.1 (Explicit activation bound and chart wall)**.** *With $r_\sigma \le \pi$ and $g \le 1$, on any domain with $\bar\sigma \le \bar\sigma_{\max}$, $\lambda \le \lambda_{\max}$, $I_{\text{gate}} \le \zeta_0$, $|\Delta A_R| \le \Delta_{\max}$:*

$$|A_{\text{fold}}| \le (c_0 - c_1\gamma)\lambda_{\max} + c_1 k_\sigma \pi \bar\sigma_{\max} + c_1\zeta_0 + \Delta_{\max} + a_0, \tag{4.4}$$

and the chart-wall supremum is explicit,

$$Q_\pi^{*,\sup} = \max\left\{ \frac{c_1 k_\sigma \pi \bar\sigma_{\max} + c_1\zeta_0 - a_0}{b},\ \frac{c_0 - c_1\gamma}{2c_1\eta_{\text{fold}}} \right\} < \infty, \tag{4.5}$$

so the Standing Hypothesis of the first Addendum reads $q_{\max}^2 \ge Q_\pi^{*,\sup}$. (Illustratively $Q_\pi^{*,\sup} = 0.85$, dominated by the peak-independent asymptote.)

Lemma 4.1 (The price in c_Ψ)**.** *Admitting full-measure peaks enlarges the resistance ceiling to $C_\sigma = \pi\bar\sigma_{\max}$, and the constant $c_\Psi = \min_{(0,C_\sigma]} T^2/\Psi_\sigma$ degrades accordingly — explicitly and finitely. With $\kappa = 2$, $\bar\sigma_{\max} = 0.8$: c_Ψ falls from 1.794 to 0.461 (factor 0.257), hence κ_σ shrinks by the same factor but remains strictly positive. The full cup costs contraction speed, never contraction itself.*

4.3 The fold-jump lemma

Standing Hypothesis 4.1 (Update-map compatibility)**.**

$$\boxed{\beta\,\eta_\sigma\,\bar\sigma_{\max} \ \le\ q^*\,\eta_\Omega} \tag{4.6}$$

— the share of metabolised resistance returned as *active* Sophia is covered by the simultaneous enlargement of the Brim.

Lemma 4.2 (Fold-jump: domain preservation and bounded jump)**.** *Under Hypothesis 4.1 and Proposition 4.1:*

(1) ***Epektasis wall.*** *The update* (4.2) *satisfies the exact identity*

$$\big(\lambda^+ - q^*\Omega_P^+\big) - \big(\lambda^- - q^*\Omega_P^-\big) = Q_{\text{fold}}\big(\beta\eta_\sigma\bar\sigma - q^*\eta_\Omega\big) \le 0, \tag{4.7}$$

(verified symbolically), so $\lambda^- \le q^*\Omega_P^-$ implies $\lambda^+ \le q^*\Omega_P^+$ for every $Q_{\text{fold}} \ge 0$.

(2) ***Remaining walls.*** *$\bar\sigma$ decreases (resistance ceiling respected); q_{fold} is continuous through $\mathfrak{F}$, so $q_{\text{fold}}^+ \in [0, q_{\max}]$; the chart target jumps boundedly, $|\Delta Q_{\text{fold}}^*|$ finite by Proposition 4.1. Hence $x^- \in \mathcal{D}_A^{\text{fold}} \Rightarrow x^+ \in \mathcal{D}_A^{\text{fold}}$.*

(3) ***Bounded certificate jump.*** *All updated quantities change by bounded multiplicative or additive amounts proportional to $Q_{\text{fold}} \le Q_\pi^{*,\sup}$, so there is a finite J_F with $\widetilde{\mathcal{L}}_{\text{ext}}(x^+) \le \widetilde{\mathcal{L}}_{\text{ext}}(x^-) + J_F$. (Numerically along both cascade branches: $\max|\Delta\lambda| \le 1.5\times10^{-3}$, $\max|\Delta\Omega_P| \le 6.3\times10^{-2}$, $\max|\Delta Q_{\text{fold}}^*| \le 0.13$.)*

Remark (Chart rebase at $\mathfrak{F}$). Because γ jumps, $\Lambda_c = \gamma/\delta$ jumps, and the normalised chart coordinates ($h_3 = 1 - \Lambda_c/\Omega_P$, r) jump even though the physical state $(u, \sigma, \lambda, \Omega_P)$ is continuous in the non-updated entries. This is a coordinate rebase, not a dynamical discontinuity: the walls are to be re-evaluated in physical variables at t_F^+, which Lemma 4.2 does.

4.4 Survival of the contraction rate

This is the genuinely new obligation: $\mathfrak{F}$ changes the parameters from which C_1 is built (γ enters κ_σ through Λ_c in $\Omega_{\min}$ and through the margin). An unbounded drift would silently destroy the theorem.

Lemma 4.3 (Product-drift bound)**.** *For $x_j \in [0, x_{\max}]$, $x_{\max} < 1$: $\prod_j (1 - x_j) \geq \exp\big(-\sum_j x_j/(1 - x_{\max})\big)$. (Verified on 2000 random sequences; minimal slack $+1.5 \times 10^{-5}$.)*

Proposition 4.2 (C_1 survives the cascade)**.** *Under fuel dominance ($\eta_\sigma > \eta_k$) the cascade dichotomy gives, on every branch, a finite total intensity $S := \sum_j Q_{\text{fold},j} < \infty$ (extinction: finite metabolic budget; permanence: finitely many events). Hence by Lemma 4.3*

$$\gamma_\infty \;\geq\; \gamma_0\, e^{-\eta_\gamma S/(1-\eta_\gamma Q_{\max})} > 0, \qquad k_{\sigma,\infty} \;\leq\; k_{\sigma,0}\, e^{\eta_k S} < \infty, \tag{4.8}$$

so Λ_c stays bounded away from zero, $\Omega_{\min}$ and the margin stay positive, and

$$\boxed{C_1^{\inf} := \inf_j \min\{\kappa_{\sigma,j}, \kappa_\Delta\} > 0} \tag{4.9}$$

uniformly along the entire hybrid trajectory ($\kappa_\Delta = 2a\mu_*$ is untouched by $\mathfrak{F}$). Numerically the exponential bound is tight*: along the extinction branch (31 events, $S = 0.517$) the actual $\gamma_{31} = 0.3938$ equals the bound to four digits, and $\kappa_\sigma : 0.0615 \to 0.0606$; along the permanence branch $\kappa_\sigma \to 0.0609$ (Figure 4.1, left).*

> The finite metabolic budget of the forced-folding cascade is exactly what keeps the contraction alive: the Vessel cannot metabolise enough resistance to undermine its own cleansing rate. Crisis spends a finite currency; C_1 is not that currency.

4.5 Hysteresis and the joint non-Zeno dwell

Resets are exogenous; forcing events are *state-triggered* (upward crossings of $A_{\text{fold}} = 0$), and the update itself moves A_{fold}. This is a genuine Zeno risk, and it is real, not hypothetical:

Definition 4.1 (Event machine with hysteresis)**.** A forcing event arms when $A_{\text{fold}} < -\varepsilon$, fires at the next upward crossing $A_{\text{fold}} = 0$, applies $\mathfrak{F}$ at the local maximum of A_{fold} on that excursion, and disarms until $A_{\text{fold}} < -\varepsilon$ again. The band $\varepsilon \geq 0$ is the hysteresis width.

Proposition 4.3 (Chatter without the band; dwell with it)**.** *Let the resistance wave be quasi-periodic with a fast component whose slope in A_{fold} exceeds the slow component's (so the rising flank carries local maxima). With $\varepsilon = 0$, the downward jump of A_{fold} at each $\mathfrak{F}$ (the fuel cut $\partial A_{\text{fold}}/\partial\bar{\sigma} \cdot m_F$) re-arms the machine between fast crests, and a* chatter chain *of events runs along the threshold band: in the verified simulation, clusters of 2–3 events at gaps $\approx 0.121 = 1/f_{\text{fast}}$ (Figure 4.1, right). With*

$$\boxed{\varepsilon \;>\; \sup_{\text{events}} |\Delta A_{\text{fold}}|_{\mathfrak{F}} \;=\; \sup\, c_1 k_\sigma\, r_\sigma\, m_F + O(\eta_a, \eta_\gamma)} \tag{4.10}$$

re-arming on the rising flank is impossible, the chain collapses to one event per slow peak, and the inter-event dwell is bounded below by the slow-wave structure: in the same simulation the minimal fold–fold gap rises from 0.121 to 2.246 (a factor 18.5), and the minimal gap over the union *of resets and foldings is 1.71.*

Standing Hypothesis 4.2 (Joint dwell)**.** The hysteresis band satisfies the bound of Proposition 4.3, and the exogenous resets respect the base dwell; then the union of $\mathfrak{R}$- and $\mathfrak{F}$-events admits a common $\Delta t_* > 0$.

The band ε is a modelling regularisation, but not an arbitrary one: its sufficient size is computable from the update map itself ($\sup|\Delta A_{\text{fold}}|_{\mathfrak{F}}$), so the non-Zeno property is restored by a constant the theory already owns.

4.6 The embodied Sophia is balance-bounded

Lemma 4.4 (Free bound for λ_{form})**.** *The three-term balance holds at flow level ($\frac{d}{dt}(\sigma + \lambda + \lambda_{\text{form}}) = I_{\text{gate}}$), through every $\mathfrak{F}$ (the m_F-split of* (4.2) *conserves the sum exactly), and through every $\mathfrak{R}$ (the metabolism m_R transfers $\sigma \to \lambda$; λ_{form} inert). Hence with $\lambda, \sigma \geq 0$,*

$$\lambda_{\text{form}}(t) \;\leq\; \sigma + \lambda + \lambda_{\text{form}} \;=\; C_0 + \mathcal{G}_{\text{recepta}}(t) \;\leq\; C_0 + \mathcal{G}^{\max}_{\text{recepta}}, \tag{4.11}$$

bounded by the grace budget: no certificate weight for λ_{form} is needed. (Verified: jump-level conservation to machine precision, 10^{-16}; full hybrid run drift $\sim 10^{-7}$, pure integrator error; $\lambda^{\max}_{\text{form}} = 0.089 \ll C_0 + \int I_{\text{gate}}$.)

4.7 Reset–fold consistency

Lemma 4.5 (The two jump maps are compatible)**.** *$\mathfrak{R}$ leaves q_{fold} and λ_{form} inert and conserves the triad ($\sigma^+ + \lambda^+ = \sigma^- + \lambda^-$); $\mathfrak{F}$ leaves q_{fold} continuous and conserves the triad by construction. Both maps preserve $\mathcal{D}_A^{\text{fold}}$ (base reset lemma; Lemma 4.2); the chart rebase occurs only at $\mathfrak{F}$ (only $\mathfrak{F}$ changes γ). Any interleaving of the two event types therefore preserves the balance, the domain, and the bounded-jump property, with jump constant $J := \max\{J_R, J_F\}$.*

4.8 Main theorem

Theorem 4.1 (Forward completeness with two jump types)**.** *Assume: the π-chart wall $q_{\max}^2 \geq Q_\pi^{*,\sup}$ (Proposition 4.1); update-map compatibility (Hypothesis 4.1); fuel dominance $\eta_\sigma > \eta_k$; and the joint dwell (Hypothesis 4.2). Then along any admissible hybrid trajectory with both Resurrectio resets and forced-folding events:*

(i) the state remains in $\mathcal{D}_A^{\text{fold}}$ and the balance $\sigma + \lambda + \lambda_{\text{form}} = C_0 + \mathcal{G}_{\text{recepta}}$ holds for all t;

(ii) the contraction rate is uniformly positive, $C_1^{\text{inf}} > 0$ (Proposition 4.2), and on every continuous arc $\dot{\widetilde{\mathcal{L}}}_{\text{ext}} \leq \widetilde{C}_{\text{ext}}^{\sup} - C_1^{\text{inf}} \widetilde{\mathcal{L}}_{\text{ext}}$ with $\widetilde{C}_{\text{ext}}^{\sup} < \infty$ (the drifting constants converge, Proposition 4.2 and Lemma 4.1);

(iii) every jump obeys $\widetilde{\mathcal{L}}_{\text{ext}}(x^+) \leq \widetilde{\mathcal{L}}_{\text{ext}}(x^-) + J$, $J = \max\{J_R, J_F\} < \infty$ (Lemmas 4.2, 4.5);

(iv) hence, with the joint dwell,

$$\boxed{\widetilde{\mathcal{L}}_{\text{ext}}(t) \;\leq\; \widetilde{L}_{**} := \max\Big\{\widetilde{\mathcal{L}}_{\text{ext}}(0),\, \widetilde{C}_{\text{ext}}^{\sup}/C_1^{\text{inf}}\Big\} + J \quad \textit{for all } t,} \tag{4.12}$$

events do not accumulate, and the trajectory is forward complete.

Grace and crisis enter only the constants $\widetilde{C}_{\text{ext}}^{\sup}$ and J; never the contraction rate.

Sketch. (i) is Lemmas 4.2, 4.4, 4.5 plus the base Nagumo invariance. For (ii), the arc estimate of the first Addendum holds with the instantaneous constants; by Proposition 4.2 the parameter sequence converges with $\inf \kappa_{\sigma,j} > 0$ and bounded $k_{\sigma,j}$, so the constants admit uniform bounds C_1^{inf}, $\widetilde{C}_{\text{ext}}^{\sup}$ valid on all arcs. (iii) is the bounded-jump property. (iv) is the standard hybrid induction: on each arc $\widetilde{\mathcal{L}}_{\text{ext}}$ decays toward $\widetilde{C}_{\text{ext}}^{\sup}/C_1^{\text{inf}}$ or below its entry value; each jump adds at most J; the joint dwell forbids accumulation; the bound follows by induction over events. □

4.9 Compact summary

$$\boxed{q_{\max}^2 \geq Q_\pi^{*,\sup} \text{ (explicit)}; \qquad c_\Psi(\pi\bar{\sigma}_{\max}) > 0 : \text{ the full cup costs speed, never contraction.}}$$

$$\boxed{\beta\eta_\sigma\bar{\sigma}_{\max} \leq q^*\eta_\Omega \;\Rightarrow\; \mathfrak{F} \text{ preserves } \mathcal{D}_A^{\text{fold}}; \quad \widetilde{\mathcal{L}}_{\text{ext}}^{+} \leq \widetilde{\mathcal{L}}_{\text{ext}}^{-} + J_F < \infty.}$$

$$\boxed{\sum_j Q_{\text{fold},j} < \infty \text{ (dichotomy)} \;\Rightarrow\; \gamma_\infty > 0,\; k_{\sigma,\infty} < \infty \;\Rightarrow\; C_1^{\text{inf}} > 0 : \text{ the budget protects the contraction.}}$$

$$\boxed{\varepsilon > \sup|\Delta A_{\text{fold}}|_{\mathfrak{F}} \;\Rightarrow\; \text{no threshold-band chatter; joint dwell } \Delta t_* > 0.}$$

$$\boxed{\lambda_{\text{form}} \leq C_0 + \mathcal{G}_{\text{recepta}}^{\max} \text{ for free, from the balance.}}$$

$$\boxed{\widetilde{\mathcal{L}}_{\text{ext}}(t) \leq \widetilde{L}_{**} < \infty \text{ with two jump types; forward complete; grace and crisis enter constants only.}}$$

V.F.S. v2.0 (Open-Gate) · Forced-Folding Lyapunov Addendum II. Extends the hybrid stability theorem to the forced-folding event type: explicit π-chart wall, fold-jump lemma with the closed-form compatibility condition, survival of C_1 through the cascade's finite metabolic budget, hysteresis non-Zeno (chatter exhibited and cured), balance-bound for λ_{form}, and reset–fold consistency. All quantitative claims verified numerically; the drift bound is tight. The hysteresis band and the update coefficients remain modelling inputs; the conclusions are domain-conditional set stability with partial convergence, never global.

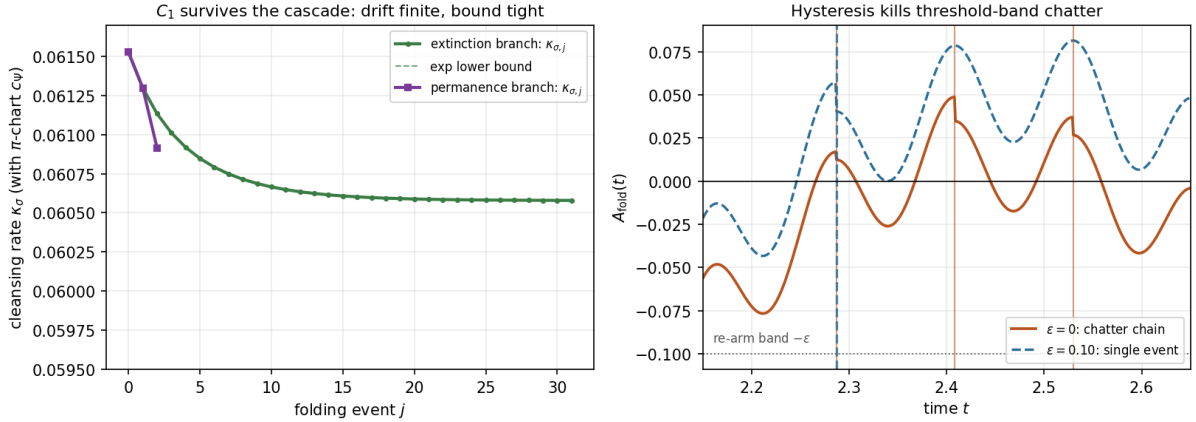

Figure 4.1: Left: survival of the cleansing rate $\kappa_{\sigma,j}$ (computed with the π-chart c_Ψ) along both terminal branches of the forced-folding cascade; the exponential lower bound of Proposition 4.2 overlays the actual sequence — tight to four digits. The drift is finite because the metabolic budget is. Right: the Zeno mechanism and its cure. With $\varepsilon = 0$ (solid) the update's downward A_{fold}-jump re-arms the event machine between fast crests of the quasi-periodic resistance wave, producing a chatter chain of three events at gaps ≈ 0.12; with $\varepsilon = 0.10$ (dashed) the band swallows the re-arming and a single event per slow peak remains — the minimal dwell grows by a factor 18.5. Parameters illustrative.

Part II

Structure Formation on the Vessel

Chapter 5

Structure Formation on the Vessel

Scope and epistemic status

Every layer so far has been spatially *homogeneous*: the Vessel is a $2{+}1$ open FLRW background $a(t) = \Omega_P(t)$ with a time-only Sophia field $\lambda(t)$. This note opens the inhomogeneous sector — how local concentrations of Sophia and form grow or decay on the expanding hyperbolic surface. As in the parent files, *Propositions* are closed-form results and *Corollaries* are interpretive. The analysis is at the linear, test-field level on a fixed background; metric back-reaction is a named next layer. Two transport constants (D for Sophia, D_q for form) are introduced; they are *new* modelling inputs, absent from the base dynamical system, and are flagged as such.

The background is

$$ds^2 = -dt^2 + \Omega_P(t)^2\, h_{ij}\, dx^i dx^j, \qquad K_h = -1, \qquad H = \frac{\dot{\Omega_P}}{\Omega_P} = \frac{\alpha\lambda}{\Omega_P}, \qquad \dot{\Omega_P} = \alpha\lambda, \tag{5.1}$$

with h the metric of the hyperbolic spatial surface $\mathbb{H}^2$.

5.1 The relaxational thesis: which field can carry structure

In standard cosmology, density structure grows by gravitational instability because the matter field carries inertia: a second-order-in-time wave equation with a sound speed permits oscillation and Jeans-unstable growth. The Sophia field of V.F.S. is different in kind. Its production law is *first order in time*,

$$\dot{\lambda} = (\delta u - \gamma)\tanh(\kappa\sigma) + I_{\text{gate}} - \eta_{\text{fold}} q_{\text{fold}}^2 \lambda, \tag{5.2}$$

a relaxation (reaction) law with no kinetic term and no spatial derivatives. Promoting it to a field on space cannot manufacture inertia; the faithful promotion of a first-order reaction law with spatial transport is a *reaction–diffusion* (parabolic) equation, not a wave (hyperbolic) one.

Proposition 5.1 (No gravitational-collapse channel in the Sophia sector)**.** *Because λ is relaxational, its linear inhomogeneities obey a parabolic equation with a real, non-oscillatory spectrum. There is no Jeans-type instability and no gravitational-collapse route to structure in the Sophia sector. Any structure on the Vessel must arise from a different, bistable order parameter.*

V.F.S. does not form structure the way ΛCDM does. Sophia is relaxational, not inertial, so it can only smooth itself out. The only route to structure is morphological symmetry breaking — the folding field (§4).

5.2 Sophia-density perturbations: reaction–diffusion on the expanding $\mathbb{H}^2$

Write $\lambda(t,x) = \bar{\lambda}(t) + \delta\lambda(t,x)$ and linearise about the homogeneous trajectory. With a phenomenological Sophia transport coefficient $D \geq 0$, and noting that physical gradients on the comoving surface redshift by Ω_P^{-2},

$$\partial_t \delta\lambda = F_\lambda(t)\,\delta\lambda + \frac{D}{\Omega_P^2}\,\Delta_h\,\delta\lambda, \qquad F_\lambda = \frac{\partial\dot{\lambda}}{\partial\lambda} = -\Gamma_\lambda, \quad \Gamma_\lambda \geq 0, \tag{5.3}$$

where $\Gamma_\lambda = \gamma + \eta_{\text{fold}} Q_{\text{fold}}$ is the local Sophia relaxation rate (the same rate whose folding-enhancement $\Gamma_\lambda = \gamma + \eta_{\text{fold}} Q_{\text{fold}}$ was found in the stability analysis). The Laplace–Beltrami operator on $\mathbb{H}^2$ has purely continuous spectrum with a gap,

$$\boxed{-\Delta_h\, Y_k = \left(\tfrac{1}{4} + k^2\right) Y_k, \qquad k \in [0,\infty),} \tag{5.4}$$

the celebrated spectral gap $\frac{1}{4}$ of the hyperbolic plane (no mode has eigenvalue below $\frac{1}{4}$). Each mode then evolves by

$$\dot{\delta\lambda}_k = s_k(t)\,\delta\lambda_k, \qquad \boxed{s_k(t) = -\Gamma_\lambda(t) - \frac{D\left(\frac{1}{4} + k^2\right)}{\Omega_P(t)^2}.} \tag{5.5}$$

Proposition 5.2 (Linear homogenisation)**.** *For $\Gamma_\lambda \geq 0$ and $D \geq 0$ every mode has $s_k < 0$: all Sophia inhomogeneities decay. The Vessel homogenises at the linear level. Moreover the hyperbolic gap supplies a minimum diffusive damping $D \cdot \frac{1}{4}/\Omega_P^2 > 0$ even for the smoothest mode $k = 0$: negative spatial curvature actively resists the largest-scale inhomogeneity.*

Integrating,

$$\delta\lambda_k(t) = \delta\lambda_k(0)\,\exp\!\left[-\int_0^t \Gamma_\lambda\,dt' - D\left(\tfrac{1}{4} + k^2\right)\mathcal{I}(t)\right], \qquad \mathcal{I}(t) := \int_0^t \frac{dt'}{\Omega_P(t')^2}. \tag{5.6}$$

Proposition 5.3 (Finite diffusive smoothing budget)**.** *Under sustained Open-Gate inflow $\lambda \to \lambda_\infty > 0$, the late-time scale factor grows linearly, $\Omega_P \sim \alpha\lambda_\infty t$, so the diffusion integral converges:*

$$\boxed{\mathcal{I}_\infty = \int_0^\infty \frac{dt}{\Omega_P^2} < \infty.} \tag{5.7}$$

Hence diffusion can suppress a mode by at most the finite factor $\exp[-D(\frac{1}{4}+k^2)\mathcal{I}_\infty]$: the expanding Vessel has a finite total smoothing budget, a comoving analogue of a damping (Silk-like) scale.

This yields two asymptotic fates, set entirely by the reaction rate Γ_λ:

1. **Generic ($\gamma > 0$).** The reaction integral $\int \Gamma_\lambda\,dt \to \infty$ dominates after diffusion saturates; *all* modes decay to zero. Complete homogenisation.
2. **Margin-stalled ($\Gamma_\lambda \to 0$).** On the active margin where cleansing stalls ($m_* \to 0$, $\inf C_1 = 0$ in the Lyapunov layer), the reaction integral is finite and the modes *freeze* at a scale-dependent residual,
$$\frac{\delta\lambda_k(\infty)}{\delta\lambda_k(0)} = \exp\!\left[-D\left(\tfrac{1}{4} + k^2\right)\mathcal{I}_\infty\right], \tag{5.8}$$
small scales (high k) erased, large scales (down to the $\frac{1}{4}$ floor) preserved — a frozen inhomogeneity spectrum with a characteristic scale $k_{1/2} \sim \mathcal{I}_\infty^{-1/2}$.

Corollary 5.1 (The smooth Vessel)**.** *Linearly, Sophia structure cannot grow; the Vessel either homogenises completely (sustained cleansing) or freezes a smooth, large-scale residual (stalled margin). There is no spontaneous Sophia clumping.*

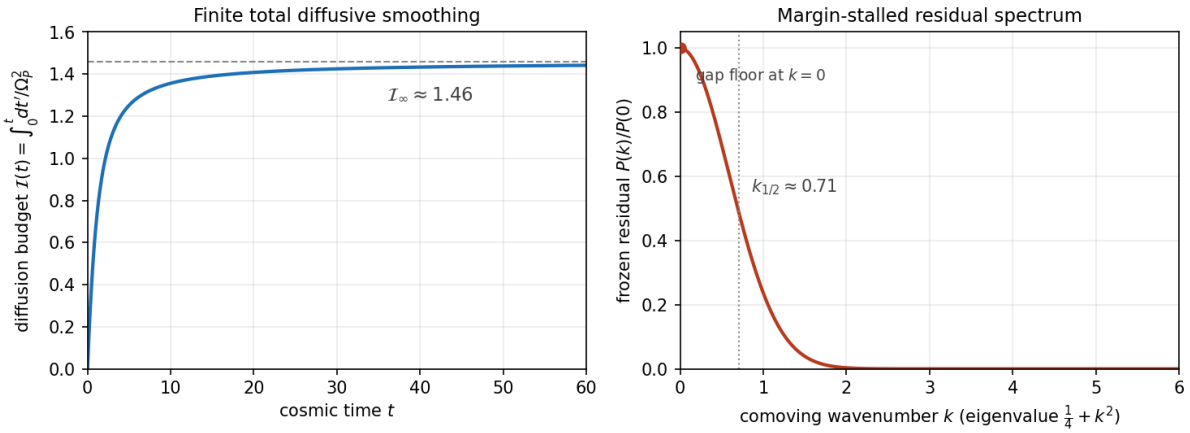

Figure 5.1: Left: the diffusive smoothing budget $\mathcal{I}(t) = \int_0^t dt'/\Omega_P^2$ saturates to a finite $\mathcal{I}_\infty$ (illustrative background $\lambda_0 = 0.4 \to \lambda_\infty = 1$, $\Omega_P(0) = 1$). Right: the margin-stalled frozen residual spectrum $P(k)/P(0)$ (with $D = 0.5$): the hyperbolic gap leaves a $k = 0$ floor while small scales are erased, defining a structure scale $k_{1/2} \approx 0.71$. Parameters illustrative.

5.3 Folding as the order parameter: pattern formation on the Vessel

By Proposition 5.1 structure must come from the bistable folding field. Promote $q_{\text{fold}} \to q_{\text{fold}}(t, x)$ with its Landau gradient dynamics plus transport:

$$\boxed{\partial_t q_{\text{fold}} = A_{\text{fold}}\, q_{\text{fold}} - B_{\text{fold}}\, q_{\text{fold}}^3 + \frac{D_q}{\Omega_P^2}\, \Delta_h\, q_{\text{fold}}.} \tag{5.9}$$

This is a real Ginzburg–Landau / Allen–Cahn equation on the expanding hyperbolic surface, invariant under the morphological reflection $q_{\text{fold}} \to -q_{\text{fold}}$ ($\mathbb{Z}_2$ symmetry, the two orientations of the fold).

Proposition 5.4 (Symmetry-breaking transition)**.** *The homogeneous state $q_{\text{fold}} = 0$ is stable for $A_{\text{fold}} < 0$. At $A_{\text{fold}} = 0$ it undergoes the supercritical pitchfork (the folding bifurcation), and for $A_{\text{fold}} > 0$ two homogeneous phases $q_{\text{fold}} = \pm\sqrt{A_{\text{fold}}/B_{\text{fold}}}$ become stable. A field initialised near $q_{\text{fold}} = 0$ over an extended Vessel then partitions into domains of $+q_*$ and $-q_*$ separated by walls on which $q_{\text{fold}} = 0$.*

These domain walls are the structure: loci of *unfolded* (old) morphology embedded in a folded Vessel — topological defects of the broken $\mathbb{Z}_2$.

Proposition 5.5 (Wall width and tension)**.** *A static planar wall has profile $q_{\text{fold}} = q_* \tanh\!\big(\xi/(\sqrt{2}\,\ell)\big)$ in physical proper distance ξ, with*

$$\boxed{\ell_{\text{phys}} = \sqrt{\frac{D_q}{A_{\text{fold}}}}\ \ (\Omega_P\text{-independent}), \qquad \tau \sim \sqrt{D_q}\,\frac{A_{\text{fold}}^{3/2}}{B_{\text{fold}}}.} \tag{5.10}$$

The physical thickness is set by the diffusion-to-reaction ratio and does not stretch with expansion; deeper folding (larger A_{fold}) makes thinner, higher-tension walls.

Sketch. In comoving coordinates the static balance is $\frac{D_q}{\Omega_P^2}\partial_x^2 q_{\text{fold}} = -A_{\text{fold}} q_{\text{fold}} + B_{\text{fold}} q_{\text{fold}}^3$, the standard quartic kink with comoving width $\ell_{\text{com}} = \Omega_P^{-1}\sqrt{D_q/A_{\text{fold}}}$; the proper width $\ell_{\text{phys}} = \Omega_P\,\ell_{\text{com}} = \sqrt{D_q/A_{\text{fold}}}$. The tension is the kink action $\int(\frac{1}{2}D_q|\partial q_{\text{fold}}|^2 + \mathcal{E}_{\text{fold}})$, giving the quoted scaling. □

Corollary 5.2 (Coarsening of the fold network)**.** *Allen–Cahn walls move by mean curvature, $v_n = -M\,\kappa_{\text{curv}}$ with mobility $M \sim D_q/\Omega_P^2$, so the domain network coarsens; simultaneously Hubble flow stretches comoving separations. Structure on the Vessel is therefore a* coarsening domain-wall network *whose characteristic scale grows by both curvature-driven merging and expansion, modified by the underlying $K_h = -1$ geometry (wall geodesics diverge on $\mathbb{H}^2$, accelerating coarsening relative to the flat case).*

The picture is sharp: the folding bifurcation is a phase transition that shatters the Vessel into oriented folded domains; the unfolded walls are the structure; they then coarsen on the expanding hyperbolic surface. This is morphological structure, born of symmetry breaking, not of gravitational clumping.

5.4 Cosmological back-reaction of the fold network

A wall network feeds back on the homogeneous budget. In $2{+}1$ dimensions a wall is a one-dimensional line in two-dimensional space; a scaling network with one wall per Hubble scale has length $\mathcal{L}_{\text{wall}} \sim \Omega_P$ over area $\sim \Omega_P^2$, so

$$\rho_{\text{wall}} \sim \frac{\tau\, \mathcal{L}_{\text{wall}}}{\Omega_P^2} \propto \Omega_P^{-1}. \tag{5.11}$$

Matching to the $2{+}1$ dilution law $\rho \propto a^{-2(1+w)}$ gives

$$\boxed{w_{\text{wall}} = -\tfrac{1}{2}.} \tag{5.12}$$

The fold network thus contributes a mildly negative-pressure component, intermediate between dust ($w = 0$) and the cosmological-constant/de Sitter limit ($w = -1$). It adds to the reconstructed $w_{\text{eff}}(t)$ a folding-structure term that is distinct from the smooth quintessence of the homogeneous Theosis branch.

Corollary 5.3 (Link to the energy-condition question)**.** *Because the network carries $w_{\text{wall}} = -\frac{1}{2} > -1$, it is NEC- and WEC-respecting: folded structure is ordinary, non-exotic content. This is the inhomogeneous face of "form makes grace lawful" — where a homogeneous Sophia surge can drive w below -1 (phantom-like, NEC-violating), the embodiment of that excess into a wall network contributes ordinary $w = -\frac{1}{2}$ matter.*

5.5 Open sub-problems and scope

1. **Metric back-reaction.** Lift from test-field to coupled perturbations: let $\delta\lambda$ and q_{fold} source the reconstructed stress tensor and solve the $2{+}1$ scalar perturbation equations. Expected to preserve Proposition 5.1 (relaxational $\Rightarrow$ no instability) but to dress the wall tension with a geometric self-energy.
2. **Coarsening law.** Derive the domain scale $L(t)$ explicitly on expanding $\mathbb{H}^2$: solve the competition between curvature-driven merging ($L^2 \sim \int M\, dt$) and Hubble stretching, with the hyperbolic correction of Corollary 5.2.
3. **Resurrectio and the network.** A reset rescales Ω_P and shifts A_{fold}; it can quench ($A^+_{\text{fold}} < 0$) or trigger ($A^+_{\text{fold}} > 0$) folding globally, i.e. dissolve or nucleate the entire wall network at a death. The hybrid network history is piecewise-coarsening with reset-induced nucleation events.
4. **Transport constants.** D and D_q are new inputs; a principled derivation (e.g. from a spatial coupling already implicit in the synergy $u = \sqrt{VF + \varepsilon}$) would remove the phenomenological freedom.

Scope. Linear, test-field, single-mode folding, fixed background. The conclusions are: (i) Sophia structure cannot grow (relaxational, homogenising); (ii) structure is morphological — a $\mathbb{Z}_2$ domain-wall network from the folding transition; (iii) the network back-reacts as $w = -\frac{1}{2}$ content. All results inherit the domain-conditional, non-global character of the underlying stability theory.

V.F.S. v2.0 (Open-Gate) · Structure Formation on the Vessel. Perturbation theory on the $2{+}1$ open FLRW background of the cosmological layer, with the folding field of the geometric layer as order parameter. Propositions are closed-form; corollaries interpretive. Transport constants and single-mode truncation are modelling inputs, not consequences of the base system.

Chapter 6

Spinodal Nucleation of the Fold Network

Scope and epistemic status

A triggering Resurrectio ($A^-_{\text{fold}} < 0 \to A^+_{\text{fold}} > 0$) drives the folding field through its symmetry-breaking transition and nucleates a fresh domain-wall network. This note computes the *initial* density of that network — how many walls per area are born, and at what scale — using the hyperbolic density of states. The two genuinely hyperbolic ingredients are the spectral gap $\frac{1}{4}$ of the Laplacian on $\mathbb{H}^2$ and the Plancherel measure $d\mu(k) = k\tanh(\pi k)\,dk$ that weights the available modes. As before, *Propositions* are closed-form; *Corollaries* interpretive; the single-mode Allen–Cahn truncation and D_q are modelling inputs. Two technical ingredients are verified numerically: the Plancherel moment limit and the Longuet–Higgins nodal coefficient (ratio measured/predicted $= 1.009$ on a Gaussian field).

The field obeys, in comoving coordinates on the unit hyperbolic surface ($K_h = -1$, comoving curvature radius $R_c = 1$),

$$\partial_t q_{\text{fold}} = A_{\text{fold}}\, q_{\text{fold}} - B_{\text{fold}}\, q^3_{\text{fold}} + \frac{D_q}{\Omega_P^2}\,\Delta_h\, q_{\text{fold}}, \qquad -\Delta_h Y_k = \left(\tfrac{1}{4} + k^2\right) Y_k. \tag{6.1}$$

6.1 Linear instability and the nucleation threshold

Immediately after the sudden trigger, A_{fold} jumps to $A^+_{\text{fold}} > 0$ and the homogeneous $q_{\text{fold}} = 0$ left by the previous arc is unstable. Linearising and decomposing in $\mathbb{H}^2$ eigenmodes,

$$\dot{\delta q}_k = \omega_k\, \delta q_k, \qquad \boxed{\omega_k = A^+_{\text{fold}} - \frac{D_q\left(\frac{1}{4} + k^2\right)}{\Omega_P^2}.} \tag{6.2}$$

Introduce the dimensionless trigger strength

$$\boxed{\Lambda := \frac{A^+_{\text{fold}}\,\Omega_P^2}{D_q}.} \tag{6.3}$$

The unstable band is $k < k_{\max}$ with $k^2_{\max} = \Lambda - \frac{1}{4}$ (in units where $D_q/\Omega_P^2 = 1$).

Proposition 6.1 (Nucleation threshold, distinct from the folding threshold)**.** *A spatial mode grows only if $\Lambda > \frac{1}{4}$. Hence there are two thresholds:*

- *folding threshold $A^+_{\text{fold}} > 0$ ($\Lambda > 0$): the homogeneous $q_{\text{fold}} = 0$ is unstable;*
- *nucleation threshold $A^+_{\text{fold}} > D_q/(4\Omega_P^2)$ ($\Lambda > \frac{1}{4}$): some spatial mode is unstable, so domains form.*

In the window $0 < \Lambda < \frac{1}{4}$ the Vessel folds, but uniformly: a single domain, no walls. Only above $\Lambda = \frac{1}{4}$ does a wall network nucleate.

The hyperbolic gap creates a nucleation threshold absent in flat space. A weak trigger ($0 < \Lambda < \frac{1}{4}$) folds the Vessel as a whole, with no internal structure; structure requires $\Lambda > \frac{1}{4}$.

6.2 The amplified field and its spectral moment

Starting from small initial fluctuations δq_0, each mode is amplified by $e^{\omega_k t}$, so the post-quench power spectrum is Gaussian in k,

$$S_k(t) \propto e^{2\omega_k t} \propto e^{-\beta\, k^2}, \qquad \beta = \frac{2D_q t}{\Omega_P^2} = \frac{2t}{\Omega_P^2/D_q}, \tag{6.4}$$

weighted by the hyperbolic Plancherel density of states $d\mu(k) = k\tanh(\pi k)\, dk$ (which reduces to the flat $k\, dk$ for $k \gg 1$ and is suppressed $\sim \frac{\pi}{2}k^2\, dk$ for $k \ll 1$). The relevant spectral second moment is

$$\left\langle \tfrac{1}{4} + k^2 \right\rangle = \tfrac{1}{4} + \frac{\displaystyle\int_0^\infty k^2\, e^{-\beta k^2}\, k\tanh(\pi k)\, dk}{\displaystyle\int_0^\infty e^{-\beta k^2}\, k\tanh(\pi k)\, dk}. \tag{6.5}$$

Proposition 6.2 (Hyperbolic small-scale moment)**.** *In the long-wavelength (hyperbolic-dominated) regime $\beta \gg 1$, where* $\tanh(\pi k) \approx \pi k$*,*

$$\langle k^2 \rangle \to \frac{3}{2\beta} = \frac{3\Omega_P^2}{4D_q t}. \tag{6.6}$$

Verified: the full integral with $\tanh(\pi k)$ *approaches* $3/(2\beta)$ *as* $\beta \to \infty$ *(e.g.* 0.0285 *vs* 0.0300 *at* $\beta = 50$*). The Plancherel* k^2*-suppression at small* k *is what replaces the flat* $1/\beta$ *by* $3/(2\beta)$ *and disfavours the very largest scales.*

The set time — when nonlinearity arrests growth at $q_* = \sqrt{A^+_{\text{fold}}/B^+_{\text{fold}}}$ — is the Kibble–Zurek time $t_{\text{set}} = A^{+\,-1}_{\text{fold}} \ln(q_*/\delta q_0)$, giving $\beta_{\text{set}} = 2\Lambda^{-1}L$ with the logarithmic factor $L := \ln(q_*/\delta q_0)$. Hence

$$\boxed{\left\langle \tfrac{1}{4} + k^2 \right\rangle_{\text{set}} = \frac{1}{4} + \frac{3\Lambda}{4L}.} \tag{6.7}$$

6.3 Wall density and the initial domain size

For an isotropic Gaussian field in two dimensions, the expected length of nodal lines (the walls, where $q_{\text{fold}} = 0$) per unit area is the Longuet–Higgins/Berry result

$$\boxed{n_{\text{wall}} = \frac{1}{2\sqrt{2}} \sqrt{\left\langle \tfrac{1}{4} + k^2 \right\rangle},} \tag{6.8}$$

verified numerically here to 0.9%. The initial comoving domain size is $\ell_{\text{init}} \sim 1/n_{\text{wall}}$:

$$\boxed{\ell_{\text{init}} \sim \frac{2\sqrt{2}}{\sqrt{\frac{1}{4} + \frac{3\Lambda}{4L}}} \quad (\text{units of } R_c).} \tag{6.9}$$

Proposition 6.3 (Three regimes of nucleation)**.**

(i) $\Lambda < \frac{1}{4}$*: no nucleation (uniform fold, Proposition 6.1).*

(ii) $\frac{1}{4} < \Lambda \lesssim \Lambda_*$*:* $\langle \frac{1}{4} + k^2 \rangle \to \frac{1}{4}$ *and* $\ell_{\text{init}} \to 4\sqrt{2}\, R_c$ *— the gap pins the domain size to the curvature radius; only a few curvature-scale domains form. (With* $L \approx 4$*, multi-domain structure* $\ell_{\text{init}} < R_c$ *sets in only at* $\Lambda_* \approx 42$*.)*

(iii) $\Lambda \gg \Lambda_*$*:* $\ell_{\text{init}} \sim \sqrt{4L/(3\Lambda)}\, R_c$*, i.e. in proper units* $\ell_{\text{init}}^{\text{phys}} \sim \sqrt{(D_q/A^+_{\text{fold}})\, L}$ *— the Kibble–Zurek correlation length* $\xi_+ = \sqrt{D_q/A^+_{\text{fold}}}$ *dressed by the* $\sqrt{L}$ *logarithm.*

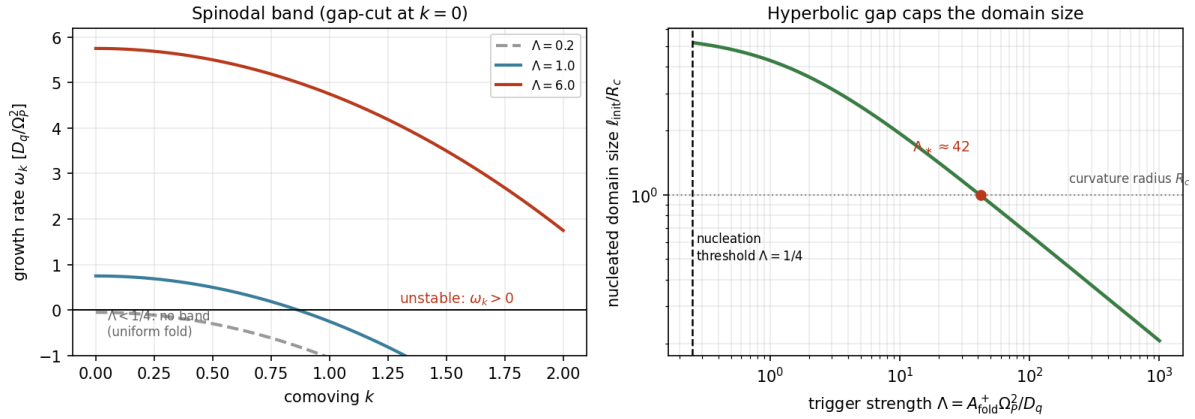

Figure 6.1: Left: linear growth rate ω_k for three trigger strengths. The Laplacian gap shifts the whole curve so that $\omega_0 = \Lambda - \frac{1}{4}$: below $\Lambda = \frac{1}{4}$ ($\Lambda = 0.2$, dashed) there is no unstable band and no nucleation. Right: the nucleated comoving domain size $\ell_{\rm init}/R_c$ versus trigger strength Λ. Near threshold the hyperbolic gap caps the size at the curvature radius (few large domains); genuine multi-domain structure ($\ell_{\rm init} < R_c$) requires $\Lambda > \Lambda_* \approx 42$; for strong triggers $\ell_{\rm init} \sim \sqrt{L/\Lambda}$ recovers the Kibble–Zurek scale. Illustrative $L = \ln(q_*/\delta q_0) = 4$.

6.4 Hyperbolic signatures

Two features distinguish nucleation on $\mathbb{H}^2$ from the flat case, both traceable to the gap and the measure:

Corollary 6.1 (Gap as a nucleation gate and a maximum domain size)**.** *The spectral gap $\frac{1}{4}$ does double duty. As an infrared cutoff it forbids weak-trigger nucleation ($\Lambda < \frac{1}{4}$: uniform fold) and caps the largest nucleated domain at the curvature radius R_c. In flat space any $A^+_{\rm fold} > 0$ nucleates and arbitrarily large domains are allowed at threshold; negative curvature both gates and bounds the structure.*

Corollary 6.2 (Measure suppression of large scales)**.** *Even within the unstable band, the Plancherel weight $k\tanh(\pi k)$ suppresses long-wavelength modes ($\sim \frac{\pi}{2}k^2$ versus the flat k), so large domains are doubly disfavoured: by the gap cutoff and by the density of states. The nucleated network is therefore finer, and more curvature-pinned, than a flat-space estimate would give.*

Interpretive: a gentle resurrection ($\Lambda < \frac{1}{4}$) re-forms the Vessel as a single undivided folded whole; only a sufficiently sharp resurrection ($\Lambda > \Lambda_*$) shatters it into many oriented domains. The negative curvature of the live domain resists fine differentiation — structure is born coarse unless the trigger is strong.

6.5 Placement and open items

This nucleation scale $\ell_{\rm init}$ is the initial condition for the intra-arc coarsening law (subproblem 2): each triggering arc begins at $\ell_{\rm init}$ (set here) and coarsens toward the frozen scale $\sqrt{\ell_0^2 + 2cD_q\mathcal{I}_\infty}$. Consistency check: the strong-trigger regime (iii) reproduces the correlation length $\xi_+ = \sqrt{D_q/A^+_{\rm fold}}$ assumed in subproblem 3, now with the Kibble–Zurek $\sqrt{L}$ dressing and the hyperbolic curvature cap.

Open items.

1. A 2D Allen–Cahn quench simulation on a hyperbolic patch to confirm the nucleated wall count $\propto \langle \frac{1}{4} + k^2 \rangle \propto \Lambda$ and fix the $O(1)$ coefficients.
2. Defect statistics beyond the mean: the distribution of initial domain areas (the Gauss–Bonnet collapse law of subproblem 2 then selects which survive).
3. The exact crossover near $\Lambda = \frac{1}{4}$ where the gap and the band compete — a hyperbolic finite-size/zero-mode analysis.

Scope. Linear spinodal stage, Gaussian-field defect counting, single-mode Allen–Cahn, sudden quench; D_q and the noise level δq_0 are modelling inputs. Results: a hyperbolic nucleation threshold $\Lambda > \frac{1}{4}$ distinct from the folding threshold; a closed-form initial wall density $n_{\text{wall}} = \frac{1}{2\sqrt{2}}\sqrt{\frac{1}{4} + 3\Lambda/4L}$; and a curvature-capped domain size interpolating from R_c (near threshold) to the Kibble–Zurek $\sqrt{(D_q/A^+_{\text{fold}})L}$ (strong trigger). The Plancherel moment and the nodal coefficient are numerically verified. Domain-conditional throughout.

V.F.S. v2.0 (Open-Gate) · Spinodal Nucleation of the Fold Network on $\mathbb{H}^2$. Linear instability of the Allen–Cahn folding field after a triggering reset, with the hyperbolic spectral gap and Plancherel measure. Propositions closed-form (Plancherel moment and Longuet–Higgins coefficient numerically verified); corollaries interpretive; transport constant and noise level are modelling inputs.

Chapter 7

Intra-Arc Coarsening of the Fold Network

Scope and epistemic status

The companion notes established that structure on the Vessel is a $\mathbb{Z}_2$ domain-wall network of the folding field and that a Resurrectio reset acts on it in three regimes, giving a sawtooth network-scale history. This note supplies the missing intra-arc piece: *between* deaths, how does the network scale $L_{\text{phys}}(t)$ evolve under pure Allen–Cahn coarsening on the expanding hyperbolic surface? No resets are involved here. As before, *Propositions* are closed-form, *Corollaries* interpretive; the single-mode Allen–Cahn truncation and the transport constant D_q are modelling inputs.

The field obeys, in comoving coordinates on the unit hyperbolic surface ($K_h = -1$),

$$\partial_t q_{\text{fold}} = A_{\text{fold}}\, q_{\text{fold}} - B_{\text{fold}}\, q_{\text{fold}}^3 + \frac{D_q}{\Omega_P^2}\, \Delta_h\, q_{\text{fold}}. \tag{7.1}$$

The folding parameters $A_{\text{fold}}, B_{\text{fold}}$ are taken quasi-stationary on the coarsening timescale (deep in a folded arc, $A_{\text{fold}} > 0$), so the dynamics is genuine coarsening of established domains rather than the initial transition.

Remark (Dimensionality matters). Allen–Cahn coarsening is curvature-driven only in two or more spatial dimensions, giving the $\ell \sim t^{1/2}$ law; in one dimension kink–antikink attraction is exponentially weak and coarsening is merely logarithmic. The 1D space–time proxy used to illustrate the reset regimes is therefore *not* representative of the true 2D coarsening rate. The present law is genuinely two-dimensional, derived via the geodesic-curvature flow on $\mathbb{H}^2$.

7.1 Wall mobility on the expanding background

In the sharp-interface limit of (7.1), a domain wall moves along its comoving normal with velocity proportional to its geodesic curvature, with a mobility set by the (comoving) diffusion coefficient:

$$v_n^{\text{com}} = -M(t)\, \kappa_g, \qquad M(t) = \frac{D_q}{\Omega_P(t)^2}. \tag{7.2}$$

The scale-factor suppression Ω_P^{-2} is the redshift of comoving gradients: as the Vessel expands, the *comoving* mobility falls, even though the proper wall structure is preserved (the proper wall width $\sqrt{D_q/A_{\text{fold}}}$ is Ω_P-independent). It is convenient to trade time for the accumulated budget already central to the smoothing analysis,

$$\mathcal{I}(t) := \int_0^t \frac{dt'}{\Omega_P(t')^2}, \qquad \frac{d}{dt} = \frac{1}{\Omega_P^2}\frac{d}{d\mathcal{I}}, \tag{7.3}$$

which is finite, $\mathcal{I} \to \mathcal{I}_\infty < \infty$, under sustained inflow ($\Omega_P \sim \alpha\lambda_\infty t$).

7.2 Gauss–Bonnet: the exact single-domain law

For a single simply-connected domain of comoving area $\mathcal{A}$ bounded by a wall undergoing geodesic curve-shortening on $\mathbb{H}^2$, the Gauss–Bonnet theorem gives the total geodesic curvature $\oint \kappa_g \, ds = 2\pi - \int_{\text{enc}} K \, dA = 2\pi + \mathcal{A}$ (since $K_h = -1$). The enclosed area therefore obeys

$$\boxed{\frac{d\mathcal{A}}{dt} = -\frac{D_q}{\Omega_P^2}\big(2\pi + \mathcal{A}\big) \quad \Longleftrightarrow \quad \frac{d\mathcal{A}}{d\mathcal{I}} = -D_q\big(2\pi + \mathcal{A}\big),} \tag{7.4}$$

with the closed-form solution

$$\boxed{\mathcal{A}(\mathcal{I}) = \big(\mathcal{A}_0 + 2\pi\big)e^{-D_q\mathcal{I}} - 2\pi.} \tag{7.5}$$

Proposition 7.1 (Survival threshold and frozen scale)**.** *A domain collapses ($\mathcal{A} = 0$) at budget $\mathcal{I}_* = D_q^{-1}\ln(1 + \mathcal{A}_0/2\pi)$. Because the total budget is finite, a domain survives the entire arc iff $\mathcal{I}_* > \mathcal{I}_\infty$, i.e.*

$$\boxed{\mathcal{A}_0 > \mathcal{A}_{\text{frozen}} := 2\pi\big(e^{D_q\mathcal{I}_\infty} - 1\big).} \tag{7.6}$$

Domains smaller than $\mathcal{A}_{\text{frozen}}$ collapse before the budget runs out; larger ones freeze into the comoving lattice. $\mathcal{A}_{\text{frozen}}$ is the characteristic frozen comoving domain area.

Proposition 7.2 (Hyperbolic acceleration)**.** *For $\mathcal{A} \gg 2\pi$ the law is $\dot{\mathcal{A}} \approx -M\mathcal{A}$: large domains collapse* exponentially*, in contrast to the flat case $\dot{\mathcal{A}} = -2\pi M$ (constant-rate Gage–Hamilton shrinking). Negative spatial curvature thus accelerates the disappearance of large domains, sharpening coarsening relative to flat space.*

In the small-budget regime $D_q\mathcal{I}_\infty \ll 1$, $\mathcal{A}_{\text{frozen}} \approx 2\pi D_q\mathcal{I}_\infty$, so the frozen comoving length is $\ell_{\text{com}} \sim \sqrt{2\pi D_q\mathcal{I}_\infty}$ — matching the scaling law below. The hyperbolic exponential (Proposition 7.2) only bites once domains grow toward the comoving curvature radius ($\mathcal{A} \sim 2\pi$), i.e. when the budget is large enough.

7.3 The network scaling law and its saturation

For the network, the standard Lifshitz–Allen–Cahn scaling $\ell\,\dot{\ell} \sim M$ becomes, on the budget variable,

$$\frac{d}{dt}\ell_{\text{com}}^2 \simeq 2c\,\frac{D_q}{\Omega_P^2} \quad \Longrightarrow \quad \boxed{\ell_{\text{com}}^2(t) = \ell_{\text{com}}^2(0) + 2c\,D_q\,\mathcal{I}(t),} \tag{7.7}$$

with an $O(1)$ constant c (consistent with Proposition 7.1, $c \sim \pi$).

Proposition 7.3 (Comoving coarsening freezes)**.** *Since $\mathcal{I}(t) \to \mathcal{I}_\infty < \infty$, the comoving domain size saturates,*

$$\ell_{\text{com}}(\infty) = \sqrt{\ell_{\text{com}}^2(0) + 2c\,D_q\,\mathcal{I}_\infty} < \infty. \tag{7.8}$$

Coarsening stops in comoving coordinates: the wall network freezes into the comoving lattice after a finite amount of merging. This is the morphological counterpart of the finite diffusive smoothing budget governing Sophia inhomogeneities — both are controlled by the same $\mathcal{I}_\infty$.

The expanding Vessel has a single finite "activity budget" $\mathcal{I}_\infty = \int dt/\Omega_P^2$. It caps both how much Sophia inhomogeneity can diffuse away and how much the fold network can coarsen. After it is spent, comoving structure is frozen.

7.4 The physical structure scale: two regimes

The proper (physical) network scale combines comoving coarsening with expansion,

$$\boxed{L_{\text{phys}}(t) = \Omega_P(t)\,\ell_{\text{com}}(t) = \Omega_P(t)\sqrt{\ell_{\text{com}}^2(0) + 2c\,D_q\,\mathcal{I}(t)}.} \tag{7.9}$$

Proposition 7.4 (Coarsening transient, then Hubble dilution)**.** *There are two regimes, separated by the budget-saturation time t_{sat} (where $\mathcal{I}$ levels):*

(i) *Early ($t \lesssim t_{\text{sat}}$): both factors grow, so L_{phys} rises faster than the scale factor — genuine coarsening on top of stretch.*

(ii) *Late ($t \gtrsim t_{\text{sat}}$): $\ell_{\text{com}} \to$ const, so $L_{\text{phys}} \to \ell_{\text{com}}(\infty)\,\Omega_P(t) \propto \Omega_P \propto t$ — pure Hubble dilution of a frozen comoving pattern.*

Coarsening is an early-time transient with a finite budget; the late-time growth of structure is expansion, not merging.

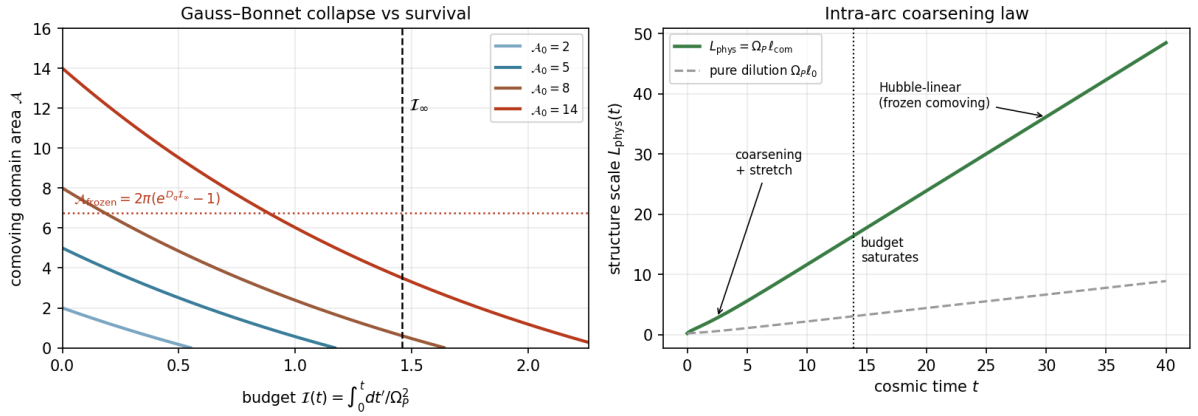

Figure 7.1: Left: Gauss–Bonnet single-domain area $\mathcal{A}(\mathcal{I})$ for several initial sizes (exact closed form, verified). Domains below $\mathcal{A}_{\text{frozen}} = 2\pi(e^{D_q \mathcal{I}_\infty} - 1)$ collapse before the finite budget $\mathcal{I}_\infty$ is spent; larger ones survive and freeze. Right: the physical structure scale $L_{\text{phys}}(t) = \Omega_P \ell_{\text{com}}$ (solid) shows an early coarsening-plus-stretch phase pulling above pure dilution $\Omega_P \ell_0$ (dashed), then a late Hubble-linear regime once the budget saturates. Background and (D_q, c) illustrative; $\mathcal{I}_\infty \approx 1.46$.

7.5 Placement in the sawtooth and open items

This intra-arc curve is the rising tooth of the hybrid sawtooth from subproblem 3: within each life-arc $L_{\text{phys}}(t)$ follows Proposition 7.4 (coarsen, then dilate), and at each death the reset acts discretely — diluting upward, refining to $\sqrt{D_q/A_{\text{fold}}}$, or erasing. Composing the intra-arc law with the reset map gives the long-run fixed-point scale, the natural next step.

Open items.

1. Determine the $O(1)$ constant c and confirm the $t^{1/2}$ (budget) law by a 2D Allen–Cahn field simulation on a hyperbolic patch with a clean structure-factor scale estimator.
2. Compose this intra-arc law with the reset map to obtain the sawtooth fixed-point structure scale, using the non-Zeno dwell time as the arc length.
3. Track the $w = -\frac{1}{2}$ wall-network contribution to the reconstructed $w_{\text{eff}}(t)$ over an arc, since $\rho_{\text{wall}} \propto \tau/\Omega_P$ with τ quasi-stationary and Ω_P growing.

Scope. Single life-arc, no resets, quasi-stationary folding parameters, single-mode Allen–Cahn; D_q a modelling input. Results: an exact Gauss–Bonnet single-domain law with a survival threshold and hyperbolic acceleration; a network scaling law $\ell_{\text{com}}^2 = \ell_0^2 + 2cD_q\mathcal{I}$ that freezes with the finite budget $\mathcal{I}_\infty$; and a physical scale L_{phys} that coarsens early and dilutes linearly late. Domain-conditional throughout.

V.F.S. v2.0 (Open-Gate) · Intra-Arc Coarsening of the Fold-Domain Network. The single-domain Gauss–Bonnet law is exact (closed form, numerically verified); the network scaling law is standard Allen–Cahn on the budget variable. Transport constant and single-mode truncation are modelling inputs; the constant c awaits a 2D field measurement.

Chapter 8

Resurrectio and the Fold-Domain Network

Scope and epistemic status

The companion note showed that structure on the Vessel is morphological: a $\mathbb{Z}_2$ domain-wall network of the folding field $q_{\text{fold}}(t, x)$, obeying the Allen–Cahn equation on the expanding hyperbolic surface. This note asks how the hybrid Resurrectio reset $\mathfrak{R}$ acts on that network. The key observation is that $\mathfrak{R}$ is *homogeneous* — it acts on the global state $(\sigma, \lambda, \Omega_P)$ — and, as established in the Lyapunov layer, it does *not* act on q_{fold}. So a reset shifts the folding potential uniformly across the whole Vessel while leaving the field configuration $q_{\text{fold}}(x)$ pointwise intact. Whether structure survives, dilutes, or is born depends on the post-reset sign of the activation index. As before, *Propositions* are closed-form; *Corollaries* interpretive; the single-mode Allen–Cahn truncation and the transport constant D_q are modelling inputs.

The network field obeys

$$\partial_t q_{\text{fold}} = A_{\text{fold}}\, q_{\text{fold}} - B_{\text{fold}}\, q_{\text{fold}}^3 + \frac{D_q}{\Omega_P^2}\, \Delta_h\, q_{\text{fold}}, \qquad q_* = \sqrt{Q^*_{\text{fold}}}, \quad Q^*_{\text{fold}} = A_{\text{fold}}/B_{\text{fold}}, \tag{8.1}$$

and the reset (geometric convention, with $m_R = (1 - q_R)\sigma^-$ the metabolised resistance) is

$$\mathfrak{R}: \quad \sigma^+ = \sigma^- - m_R, \quad \lambda^+ = \lambda^- + m_R, \quad \Omega_P^+ = \Omega_P^- + \kappa_R \mathcal{G}^-_{\text{recepta}}, \quad q_{\text{fold}} \text{ continuous}, \tag{8.2}$$

which shifts the activation index by $\Delta A_{\text{fold}} = \Theta\, m_R + c_1 \Delta I_{\text{gate}}$, $\Theta = c_0 - c_1(\gamma + k_\sigma)$, exactly as in the folding-trigger note.

8.1 Three regimes of a reset acting on the network

Because $\mathfrak{R}$ shifts A_{fold} uniformly while preserving $q_{\text{fold}}(x)$, the network's fate is fixed by the pre- and post-reset signs of A_{fold}:

Definition 8.1 (Reset regimes)**.**

(I) **Quench** ($A^-_{\text{fold}} > 0 \to A^+_{\text{fold}} < 0$): the double well collapses to a single well at $q_{\text{fold}} = 0$.

(II) **Rescale** ($A^-_{\text{fold}} > 0 \to A^+_{\text{fold}} > 0$): the wells persist with shifted depth and the scale factor jumps.

(III) **Trigger** ($A^-_{\text{fold}} < 0 \to A^+_{\text{fold}} > 0$): a single well bifurcates into a double well.

Proposition 8.1 (Regime boundaries)**.** *With $\Delta A_{\text{fold}} = \Theta m_R + c_1 \Delta I_{\text{gate}}$, a reset from A^-_{fold} produces $A^+_{\text{fold}} = A^-_{\text{fold}} + \Delta A_{\text{fold}}$. Hence, neglecting the bounded gate term: a quench requires $\Theta < 0$ and $|\Theta| m_R > A^-_{\text{fold}}$; a trigger requires $\Theta > 0$ and $\Theta m_R > |A^-_{\text{fold}}|$; otherwise the reset rescales. The folding-response coefficient Θ thus selects whether resurrection destroys, preserves, or creates morphological structure.*

A death-and-resurrection does not move the walls. It lifts or lowers the entire folding potential at once — and depending on the sign of Θ, the whole network dissolves, is re-tensioned and diluted, or is nucleated from nothing.

8.2 Quench: dissolution of the network

When $A^+_{\text{fold}} < 0$, the configuration $q_{\text{fold}}(x)$ everywhere relaxes to $q_{\text{fold}} = 0$. Linearising (8.1) about zero, each mode decays at rate $|A^+_{\text{fold}}| + D_q(\frac{1}{4} + k^2)/\Omega_P^{+2} > 0$, so the entire pattern fades on the timescale

$$\tau_{\text{dissolve}} = \frac{1}{|A^+_{\text{fold}}|}. \tag{8.3}$$

The walls do not migrate and annihilate; the whole differentiated morphology evaporates uniformly, returning the Vessel to the undifferentiated old form.

Corollary 8.1 (Death as leveling)**.** *A quench-resurrection returns the entire Vessel to the unfolded state $q_{\text{fold}} = 0$: all oriented domains are erased, all walls dissolved. Death levels morphological structure.*

8.3 Trigger: nucleation as a sudden quench (Kibble–Zurek)

When $A^-_{\text{fold}} < 0 \to A^+_{\text{fold}} > 0$, the homogeneous $q_{\text{fold}} = 0$ left behind by the previous arc becomes unstable. Since $\mathfrak{R}$ is instantaneous, A_{fold} jumps discontinuously: a *sudden quench* through the symmetry- breaking transition. Linearising about $q_{\text{fold}} = 0$ after the jump,

$$\dot{\delta q}_k = \left[A^+_{\text{fold}} - \frac{D_q(\frac{1}{4} + k^2)}{\Omega_P^{+2}}\right] \delta q_k, \tag{8.4}$$

so a band of modes $k < k_{\text{max}}$, $k^2_{\text{max}} = A^+_{\text{fold}}\Omega_P^{+2}/D_q - \frac{1}{4}$, grows and the field undergoes spinodal decomposition. The emergent (physical) domain size is the post-quench correlation length,

$$\boxed{\ell_{\text{init}} \sim \xi_+ = \sqrt{\frac{D_q}{A^+_{\text{fold}}}}} \tag{8.5}$$

the same scale as the wall width: the network is born saturated — as fine as the walls themselves — then coarsens. Deeper triggers (larger A^+_{fold}) nucleate finer networks.

Corollary 8.2 (Resurrection as individuation)**.** *A trigger-resurrection shatters the undifferentiated old form into a fine network of newly differentiated oriented domains, with the old form surviving only as the thin walls between them. Where quench levels, trigger differentiates.*

This is a Kibble–Zurek-type defect formation: the reset drives the system through a symmetry-breaking transition and freezes in a defect network whose initial scale is set by the correlation length at the transition. Here the quench is sudden, so ℓ_{init} is the spinodal scale ξ_+.

8.4 Rescale: re-tensioning and dilution

When both $A^{\pm}_{\text{fold}} > 0$, the domains persist but everything jumps. With $q_* = \sqrt{A_{\text{fold}}/B_{\text{fold}}}$, $\ell_{\text{phys}} = \sqrt{D_q/A_{\text{fold}}}$, $\tau \sim \sqrt{D_q}\, A^{3/2}_{\text{fold}}/B_{\text{fold}}$, a reset induces

$$q^+_* = \sqrt{\frac{A^+_{\text{fold}}}{B^+_{\text{fold}}}}, \qquad \frac{\ell^+_{\text{phys}}}{\ell^-_{\text{phys}}} = \sqrt{\frac{A^-_{\text{fold}}}{A^+_{\text{fold}}}}, \qquad \frac{\tau^+}{\tau^-} = \left(\tfrac{A^+_{\text{fold}}}{A^-_{\text{fold}}}\right)^{3/2} \frac{B^-_{\text{fold}}}{B^+_{\text{fold}}}, \tag{8.6}$$

and, crucially, the comoving topology is untouched while proper inter-wall separations are stretched by the scale-factor jump,

$$\boxed{L^+_{\text{phys}} = \frac{\Omega^+_P}{\Omega^-_P}\, L^-_{\text{phys}} = \Big(1 + \frac{\kappa_R \mathcal{G}^-_{\text{recepta}}}{\Omega^-_P}\Big) L^-_{\text{phys}}.} \tag{8.7}$$

The network is diluted: the same domains, spread wider.

Corollary 8.3 (Amplitude convergence under repeated rescaling)**.** *The contraction $Q^{*+}_{\text{fold}} - Q_{\text{crit}} = \kappa_{\text{fold}}(Q^{*-}_{\text{fold}} - Q_{\text{crit}})$ of the folding-trigger note drives the domain amplitude to a universal value across repeated resets, $q_* \to \sqrt{Q_{\text{crit}}}$ (when $\sum m_R = \infty$). Resurrection stabilises* how strongly *the Vessel is folded, while expansion keeps diluting* how widely.

8.5 The hybrid network history

Over a sequence of life-arcs the structure scale $L_{\mathrm{phys}}(t)$ follows a sawtooth: within each arc the network coarsens (curvature-driven merging plus Hubble stretch), and at each death it is acted on by $\mathfrak{R}$ — diluted upward (rescale), reset to the fine scale ξ_+ (trigger), or erased (quench).

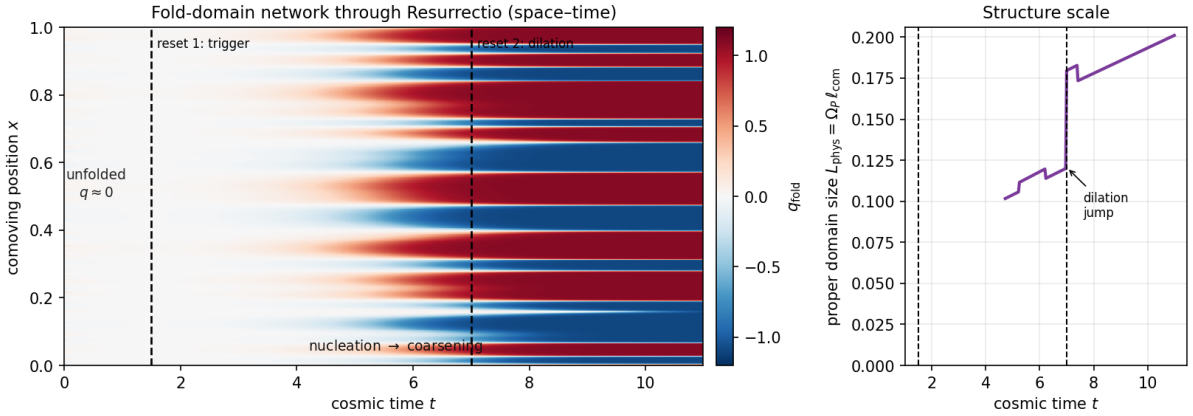

Figure 8.1: Allen–Cahn simulation of the fold-domain network through two resets (illustrative parameters; 1D comoving slice as a proxy). Left: space–time map of q_{fold}. The Vessel is unfolded ($q_{\mathrm{fold}} \approx 0$) until *reset 1* triggers the transition; domains then nucleate from fluctuations and coarsen. *Reset 2* is a rescale (regime II): the comoving pattern is untouched but the scale factor jumps. Right: the proper domain size $L_{\mathrm{phys}} = \Omega_P \ell_{\mathrm{com}}$ grows by coarsening and shows a discrete dilation jump at reset 2.

Corollary 8.4 (Resurrection as a renormalisation step on structure)**.** *Each reset is a coarse-grain (dilation, regime II) or refine (nucleation to ξ_+, regime III) operation on the network, composed with intra-arc coarsening. The long-run structure scale is the fixed point of (arc coarsening) $\circ$ (reset action); a steady balance between expansion-driven dilution and reset-driven nucleation.*

8.6 Cosmological back-reaction across resets

Within a scaling arc the wall network contributes $\rho_{\mathrm{wall}} \sim \tau/\Omega_P \propto \Omega_P^{-1}$, i.e. $w_{\mathrm{wall}} = -\frac{1}{2}$ in 2+1 dimensions (companion note). At a reset this jumps: τ changes through $A_{\mathrm{fold}}, B_{\mathrm{fold}}$ and Ω_P jumps, so

$$\frac{\rho_{\mathrm{wall}}^{+}}{\rho_{\mathrm{wall}}^{-}} = \frac{\tau^{+}}{\tau^{-}} \cdot \frac{\Omega_P^{-}}{\Omega_P^{+}}. \tag{8.8}$$

A quench sets $\rho_{\mathrm{wall}} \to 0$: the morphological energy is released back into the homogeneous Sophia budget. A trigger creates ρ_{wall} from zero: structure energy is drawn from the folding transition. Thus resurrection redistributes energy between the homogeneous (λ) and structured (wall-network) sectors — a discrete exchange invisible to the homogeneous reconstruction alone.

8.7 Reading and open items

Interpretive reading. The walls are loci of persistent unfolded (old) form. A quench- resurrection returns the whole Vessel to undifferentiated old form (death as leveling, $\Theta < 0$); a trigger-resurrection shatters that undifferentiated form into newly differentiated oriented domains, the old form surviving only as the thin boundaries between them (resurrection as individuation, $\Theta > 0$). Repeated rescaling fixes the depth of folding ($q_* \to \sqrt{Q_{\mathrm{crit}}}$) while expansion keeps widening the pattern. The sign of Θ — whether metabolised resistance promotes or suppresses form — decides which face a given resurrection wears.

Open items.

1. Quantify the spinodal nucleation density on $\mathbb{H}^2$ (hyperbolic spectral gap modifies the unstable band) and the resulting initial wall count per Hubble area.
2. Derive the sawtooth fixed-point scale explicitly from (coarsening law) $\circ$ (reset map), using the non-Zeno dwell time as the arc length.
3. Track the $\lambda \leftrightarrow$ network energy exchange as a correction to the reconstructed $w_{\text{eff}}(t)$ history, and test for a folding-induced feature near the phantom divide.

Scope. Single-mode Allen–Cahn, test-field, 1D simulation proxy; transport constant D_q a modelling input. Conclusions: a homogeneous reset acts on the morphological network in three regimes fixed by sign Θ and the jump size — dissolve, dilute, or nucleate — and resurrection functions as a renormalisation step on Vessel structure, exchanging energy between the homogeneous and structured sectors. Domain-conditional throughout.

V.F.S. v2.0 (Open-Gate) · Resurrectio and the Fold-Domain Network. Builds on the structure-formation companion (Allen–Cahn folding network on $2{+}1$ open FLRW) and the Resurrectio reset of the Lyapunov layer. Propositions closed-form; corollaries interpretive; numerical figure illustrative.

Chapter 9

The Sawtooth Fixed Point of the Fold Network

Scope and epistemic status

The three preceding notes supply the pieces: the nucleation scale ℓ_{init} at a triggering reset (subproblem 1), the intra-arc coarsening law governed by the finite budget $\mathcal{I}_\infty = \int_0^\infty dt/\Omega_P^2$ (subproblem 2), and the three-regime reset map — quench, rescale, trigger (subproblem 3). This note composes them: over a sequence of life-arcs punctuated by resets, what is the long-run network scale? The central result is that the finite coarsening budget forces the *comoving* scale to converge to a constant ℓ_* regardless of the (random) reset schedule, so the physical scale is asymptotically $L_{\text{phys}}(t) \to \ell_* \Omega_P(t) \propto t$. This also resolves the earlier worry that the random arc length would obstruct a fixed point: the finite budget makes the asymptotics universal. As before, *Propositions* are closed-form; *Corollaries* interpretive; the reduced recursion (tracking the scale, not the full field), the coarsening constant c, and the reset-regime schedule are modelling inputs.

9.1 The comoving recursion

Track the comoving network scale ℓ_{com} across arcs. Index the arcs by j; let ℓ_j be the comoving scale entering arc j and $\Delta\mathcal{I}_j = \int_{\text{arc j}} dt/\Omega_P^2$ the budget consumed during it. Within the arc, the coarsening law (subproblem 2) gives $\ell^2 \mapsto \ell^2 + 2cD_q\,\Delta\mathcal{I}_j$; at the closing reset, the regime acts:

$$\boxed{\ell_{j+1}^2 = R_j\Big(\ell_j^2 + 2cD_q\,\Delta\mathcal{I}_j\Big), \qquad R_j = \begin{cases} \text{id}, & \text{rescale (comoving topology unchanged)} \\ \ell_{\text{init}}^2, & \text{trigger (re-nucleation)} \\ \varnothing, & \text{quench (dissolve; re-nucleate at next trigger)} \end{cases}} \tag{9.1}$$

The essential constraint, inherited from the finite expansion budget, is

$$\sum_j \Delta\mathcal{I}_j \le \mathcal{I}_\infty < \infty. \tag{9.2}$$

Remark (Why rescale is the identity on the comoving scale). A rescale reset jumps Ω_P but leaves the comoving pattern intact, so it does not change ℓ_{com}; its only effect is on the physical scale, $L_{\text{phys}} = \Omega_P \ell_{\text{com}}$. The comoving recursion therefore sees rescales as no-ops, triggers as resets to ℓ_{init}, and quenches as dissolutions.

9.2 Finite budget forces convergence

Proposition 9.1 (Vanishing late-time coarsening)**.** *For any reset schedule with non-Zeno dwell $\Delta t_j \ge \Delta t_* > 0$, the per-arc coarsening increment vanishes,*

$$2cD_q\,\Delta\mathcal{I}_j \to 0 \qquad (j \to \infty), \tag{9.3}$$

because $\sum_j \Delta\mathcal{I}_j \le \mathcal{I}_\infty < \infty$ forces $\Delta\mathcal{I}_j \to 0$ (equivalently $\Delta\mathcal{I}_j \le \Delta t_j/\Omega_P^2$ with $\Omega_P \to \infty$). The random arc lengths do not affect this: the finite budget dominates.

Proposition 9.2 (Convergence of the comoving scale)**.** *The comoving scale converges to a constant ℓ_*:*

(i) if triggers recur infinitely often, each pins ℓ to ℓ_{init} and (by Proposition 9.1) the subsequent coarsening cannot grow it, so $\ell_j \to \ell_{\text{init}}$;

(ii) if all resets after some arc J are rescales, then $\ell_j^2 \to \ell_J^2 + 2cD_q\sum_{j\ge J}\Delta\mathcal{I}_j =: \ell_\infty^2 < \infty$, the frozen value.

In either case $\ell_j \to \ell_* \in [\ell_{\text{init}}, \ell_\infty]$, with $\ell_\infty = \sqrt{\ell_{\text{init}}^2 + 2cD_q(\mathcal{I}_\infty - \mathcal{I}_{\text{nuc}})}$ the maximal frozen scale (single nucleation, no retrigger).

Proposition 9.3 (Universal physical asymptotics)**.** *The physical structure scale obeys*

$$\boxed{L_{\text{phys}}(t) = \Omega_P(t)\,\ell_{\text{com}}(t) \;\longrightarrow\; \ell_*\,\Omega_P(t) \;\propto\; t,} \tag{9.4}$$

independent of the reset schedule. Different random histories differ only in the value of $\ell_* \in [\ell_{\text{init}}, \ell_\infty]$, not in the $\propto \Omega_P$ growth.

The coarsening budget is finite, so the comoving network freezes. Resurrection can *refresh* the scale (a trigger resets it to ℓ_{init}) but cannot *re-coarsen* it once the budget is spent. The late-time structure scale is a relic of the young Vessel, carried outward by pure expansion.

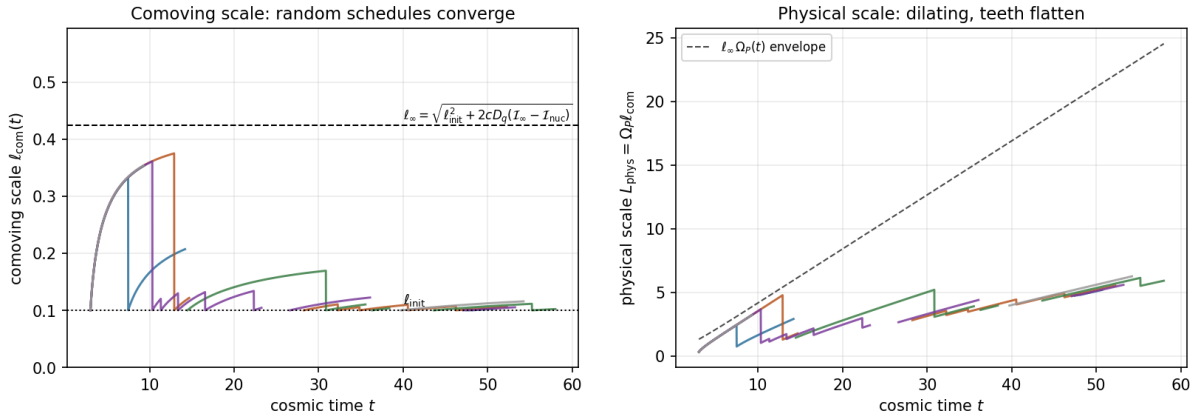

Figure 9.1: Reduced recursion over five random reset schedules (non-Zeno spacing; rescale/trigger/quench with probabilities $0.7/0.15/0.15$; illustrative $2cD_q = 0.5$, $\ell_{\text{init}} = 0.1$, $\mathcal{I}_\infty \approx 1.46$). Left: the comoving scale $\ell_{\text{com}}(t)$ — early arcs coarsen substantially toward ℓ_∞, but as the budget depletes the teeth flatten and every schedule is pinned near ℓ_{init} at late times. Right: the physical scale $L_{\text{phys}} = \Omega_P \ell_{\text{com}}$ dilates along the $\ell_\infty \Omega_P(t)$ envelope; gaps are quench intervals (network dissolved). Comoving teeth flatten; physical scale keeps dilating $\propto \Omega_P \propto t$.

9.3 Reading and consequences

Corollary 9.1 (Structure scale is a young-Vessel relic)**.** *Because coarsening is budget-limited, the comoving structure scale is set in the early, slowly-expanding era and frozen thereafter. The mature Vessel does not generate new structure scale by merging; it merely carries the early-frozen pattern outward by expansion. Any apparent late-time growth of L_{phys} is Hubble dilution, not coarsening.*

Corollary 9.2 (Resurrection refreshes but cannot re-coarsen)**.** *A late trigger-resurrection re-nucleates the network at the fine scale ℓ_{init}, and the depleted budget leaves it there: the renewed structure is permanently fine. Only resurrections occurring early, while the budget is ample, can be followed by appreciable coarsening. Early death-and-rebirth permits maturation of form; late death-and-rebirth yields perpetually fine, uncoarsened structure.*

The composition closes the programme's internal loop: subproblem 1 sets the floor ℓ_{init}, subproblem 2 sets the ceiling ℓ_∞ via the budget, subproblem 3 supplies the reset action, and the finite budget collapses the sawtooth onto $\ell_* \in [\ell_{\text{init}}, \ell_\infty]$ with universal physical asymptotics $L_{\text{phys}} \propto \Omega_P$.

9.4 Open items and scope

Open items.

1. Replace the reduced scale-recursion by a full 2D Allen–Cahn field simulation through a reset sequence, to confirm ℓ_* and the flattening of the comoving teeth.
2. Couple the reset-regime probabilities to the actual $A_{\text{fold}}(t)$ history (rising with λ via epektasis, dipped by metabolism when $\Theta < 0$), replacing the illustrative fixed probabilities by the dynamically determined regime sequence.
3. Feed ℓ_* and the wall tension into the $w = -\frac{1}{2}$ network back-reaction to obtain the folding-structure contribution to $w_{\text{eff}}(t)$ over cosmic history (link to the energy-condition direction).

Scope. Reduced recursion (network scale, not the full field); single-mode Allen–Cahn; coarsening constant c and reset-regime schedule are modelling inputs; the finite-budget convergence is robust to the random schedule. Result: the comoving network scale converges to $\ell_* \in [\ell_{\text{init}}, \ell_\infty]$ and the physical scale is universally $L_{\text{phys}} \to \ell_* \Omega_P \propto t$. Domain-conditional throughout.

V.F.S. v2.0 (Open-Gate) · The Sawtooth Fixed Point of the Fold Network. Composes the nucleation scale (subproblem 1), the budget-limited coarsening law (subproblem 2), and the three-regime reset map (subproblem 3). The convergence follows from the finite budget $\mathcal{I}_\infty$ and is robust to the random reset schedule. Propositions closed-form; corollaries interpretive; reduced recursion and coarsening constant are modelling inputs.

Chapter 10

The Transport Constants from First Principles

Scope and epistemic status

The structure-formation programme introduced two transport coefficients — a Sophia diffusivity D and a folding diffusivity D_q — as phenomenological inputs, on which all quantitative results depend. This note asks whether VFS mechanics fixes them. The answers are sharp: (i) the Sophia field has *no* fundamental diffusion, $D = 0$, because it is purely relaxational; its inhomogeneities are slaved to the folding field through the embodiment feedback. (ii) The folding diffusivity is *not* an independent constant: its spatial structure (Ω_P^{-2} and the hyperbolic $K_h = -1$) is inherited from the live-domain metric, and its single scalar magnitude is the bending stiffness of the shape-stability operator $\mathcal{L}_0$ — the gradient partner of the rigidity a_0 already in the theory. As before, *Propositions* are closed-form; *Corollaries* interpretive. The slaving relation is verified symbolically; the reduction of D_q to a single bending length still rests on the minimal one-modulus model of $\mathcal{L}_0$, which is flagged.

10.1 Sophia does not diffuse

In the base dynamical system the Sophia production law

$$\dot{\lambda} = (\delta u - \gamma)\tanh(\kappa\sigma) + I_{\text{gate}} - \eta_{\text{fold}}\, q_{\text{fold}}^2 \lambda \tag{10.1}$$

contains no spatial derivative of λ: it is a pointwise relaxation law. Promoting λ to a field therefore introduces no gradient coupling of its own.

Proposition 10.1 (Zero fundamental Sophia diffusivity)**.** *The Sophia field carries no kinetic or gradient term in the base system, so its fundamental diffusivity vanishes, $D = 0$. Linear Sophia inhomogeneities obey a pure local relaxation, $\partial_t \delta\lambda = -\Gamma_\lambda\, \delta\lambda + (\textit{folding source})$, with no k-dependent spatial transport.*

Remark (Correction to the structure-formation note). The frozen residual spectrum of the structure-formation companion assumed $D > 0$. With $D = 0$, the Sophia-only modes decay uniformly at the local rate Γ_λ with no k-dependence: on a stalled margin ($\Gamma_\lambda \to 0$) they freeze with a *flat* residual, not a scale-graded one. All scale-dependent structure is morphological, not Sophianic.

Although Sophia does not diffuse, it is not inert: the embodiment feedback $-\eta_{\text{fold}} q_{\text{fold}}^2 \lambda$ couples it to the folding field. Linearising about $(\bar{\lambda}, \bar{q})$,

$$\partial_t \delta\lambda = -\big(\Gamma_\lambda + \eta_{\text{fold}}\bar{q}^2\big)\delta\lambda - 2\eta_{\text{fold}}\bar{\lambda}\bar{q}\,\delta q_{\text{fold}}, \tag{10.2}$$

and in the quasi-static (fast-relaxation) limit

$$\boxed{\delta\lambda^* = -\frac{2\eta_{\text{fold}}\bar{\lambda}\bar{q}}{\Gamma_\lambda + \eta_{\text{fold}}\bar{q}^2}\;\delta q_{\text{fold}}.} \tag{10.3}$$

Proposition 10.2 (Sophia structure is slaved to form)**.** *Sophia inhomogeneity is a fixed multiple of folding inhomogeneity, with a bounded coefficient* $S(\bar{q}) = 2\eta_{\text{fold}}\bar{\lambda}\bar{q}/(\Gamma_\lambda + \eta_{\text{fold}}\bar{q}^2)$ *maximised at* $\bar{q} = \sqrt{\Gamma_\lambda/\eta_{\text{fold}}}$*, where* $S_{\max} = \bar{\lambda}\sqrt{\eta_{\text{fold}}/\Gamma_\lambda}$*. Sophia carries no independent structural degree of freedom: its spatial pattern is the shadow of the folding pattern.*

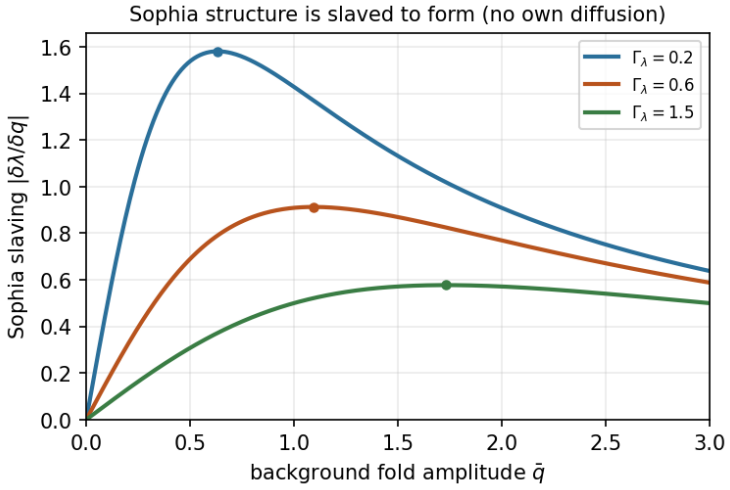

Figure 10.1: The Sophia slaving coefficient $|\delta\lambda/\delta q_{\text{fold}}| = S(\bar{q})$ (verified symbolically). It is bounded, vanishes at $\bar{q} = 0$ and at large $\bar{q}$, and peaks at $\bar{q} = \sqrt{\Gamma_\lambda/\eta_{\text{fold}}}$. Sophia inhomogeneity is sourced entirely by folding inhomogeneity; there is no independent Sophia diffusion to set. Illustrative $\eta_{\text{fold}} = 0.5$, $\bar{\lambda} = 1$.

There is really one structural field. Sophia does not diffuse; wherever the Vessel is inhomogeneous in Sophia, it is because it is inhomogeneous in *form*, and the two are locked by the embodiment feedback. The Sophia diffusivity D is not a missing constant — it is identically zero.

10.2 The folding diffusivity is geometric

The folding field's spatial coupling is fixed in two stages: its *structure* by the metric, its *magnitude* by the shape operator.

10.2.1 Structure: inherited from the live-domain metric

The folding free energy, built geometrically, measures gradients with the live-domain metric g (geometry layer, scalar curvature $-2/\Omega_P^2$, conformally hyperbolic $g = \Omega_P^2 h$):

$$\mathcal{F}[q_{\text{fold}}] = \int_\Sigma \left[\tfrac{\kappa_b}{2}\,|\nabla_g q_{\text{fold}}|^2 + \tfrac{r}{2}q_{\text{fold}}^2 + \tfrac{B}{4}q_{\text{fold}}^4\right]\sqrt{g}\,d^2x, \qquad r = a_0 - c_0\lambda - c_1\dot{\lambda} = -A_{\text{fold}}. \tag{10.4}$$

The Laplace–Beltrami operator of g is $\Delta_g = \Omega_P^{-2}\Delta_h$, so the gradient-flow dynamics $\partial_t q_{\text{fold}} = -M\,\delta\mathcal{F}/\delta q_{\text{fold}}$ is automatically

$$\partial_t q_{\text{fold}} = A_{\text{fold}}\,q_{\text{fold}} - B_{\text{fold}}\,q_{\text{fold}}^3 + \frac{M\kappa_b}{\Omega_P^2}\,\Delta_h\,q_{\text{fold}}, \qquad A_{\text{fold}} = -Mr,\ B_{\text{fold}} = MB. \tag{10.5}$$

Proposition 10.3 (The Ω_P^{-2} and $K_h = -1$ are not chosen)**.** *The redshift factor* Ω_P^{-2} *and the hyperbolic Laplacian* Δ_h *in the folding transport term are the Laplace–Beltrami operator of the live-domain metric established in the geometric layer, not modelling choices. Only a single scalar,* $D_q = M\kappa_b$*, remains free.*

10.2.2 Magnitude: the bending stiffness of $\mathcal{L}_0$

The remaining scalar is $D_q = M\kappa_b$, the product of the shape mobility M and the bending stiffness κ_b. The bending stiffness is the gradient coefficient of the very shape-stability operator $\mathcal{L}_0$ whose constant-mode eigenvalue is the rigidity a_0 (the operator whose bifurcation defines folding). In the natural time units where the uniform folding rate is A_{fold} one has $M = 1$, so $D_q = \kappa_b$, and all physical lengths depend only on the ratio

$$\boxed{\ell_b^2 := \frac{\kappa_b}{a_0} = \frac{D_q}{a_0}\,, \qquad \text{wall width} = \sqrt{\frac{D_q}{A_{\text{fold}}}} = \ell_b\sqrt{\frac{a_0}{A_{\text{fold}}}}\,.} \tag{10.6}$$

Proposition 10.4 (Folding diffusivity is the gradient partner of the rigidity)**.** *D_q is not independent of the theory's existing constants: it is the gradient coefficient of $\mathcal{L}_0$, whose constant-mode coefficient is a_0. Physical scales (wall width, nucleation scale, coarsening and frozen scales) depend only on the bending length $\ell_b = \sqrt{D_q/a_0}$, a ratio internal to $\mathcal{L}_0$. In the minimal one-modulus (Helfrich/Willmore) model of $\mathcal{L}_0$, where rigidity and bending share a single modulus, ℓ_b is fixed by the reference shape and $D_q = a_0\ell_b^2$ ceases to be a free input altogether.*

The reduction is concrete: from "an arbitrary spatial coupling plus a free constant" to "a single bending length ℓ_b, the gradient partner of the rigidity a_0 already present in $A_{\text{fold}} = c_0\lambda + c_1\dot{\lambda} - a_0$." The spatial form is pure geometry; the magnitude is the Vessel's stiffness, not a new dial.

10.3 Consequences for the programme

Corollary 10.1 (One structural field, one length)**.** *The structure-formation programme has, after this reduction, a single genuine input: the bending length $\ell_b = \sqrt{D_q/a_0}$. The Sophia diffusivity is zero; the folding transport structure is geometric; the folding magnitude is the shape stiffness. Every scale derived earlier — the nucleation size $\ell_{\text{init}} \sim \ell_b\sqrt{a_0/A^+_{\text{fold}}}\,(\ldots)$, the frozen comoving scale, the sawtooth fixed point — is expressed through ℓ_b and the already-existing folding parameters.*

Corollary 10.2 (Sophia structure rides on form)**.** *Because $\delta\lambda$ is slaved to δq_{fold} (Proposition 10.2), the Sophia inhomogeneity spectrum is the folding spectrum times the bounded factor $S(\vec{q})$. Wherever folding nucleates a domain-wall network, a matching Sophia pattern appears; where folding is quenched, Sophia re-homogenises. There is no separate Sophia structure-formation problem.*

10.4 Open items and scope

Open items.

1. Fix the bending length ℓ_b from an explicit form of the shape-stability operator $\mathcal{L}_0$ (e.g. the second variation of a Willmore/Helfrich bending energy of the live surface), turning Proposition 10.4 from a relation into a number.
2. Verify the slaving relation (Proposition 10.2) beyond the quasi-static limit, including the finite Sophia relaxation time, and check it against a coupled $(q_{\text{fold}}, \lambda)$ field simulation.
3. Propagate $D = 0$ and the slaving into the cosmological back-reaction: the Sophia-structure contribution to w_{eff} is then a fixed multiple of the wall-network contribution.

Scope. Results: the Sophia diffusivity is identically zero (relaxational field), with Sophia inhomogeneity slaved to folding via the embodiment feedback (symbolically verified); the folding transport structure is the Laplace–Beltrami operator of the live-domain metric (not a choice); and the folding magnitude reduces to the bending length $\ell_b = \sqrt{D_q/a_0}$, the gradient partner of the rigidity a_0 in $\mathcal{L}_0$. The remaining modelling freedom is the single length ℓ_b (a number only in the minimal one-modulus model). Domain-conditional throughout.

V.F.S. v2.0 (Open-Gate) · The Transport Constants from First Principles. Closes the structure-formation programme's modelling inputs: $D = 0$ with Sophia slaved to form; D_q geometric in structure and equal to the shape-operator bending stiffness in magnitude, reducible to one bending length. Propositions closed-form (slaving verified symbolically); corollaries interpretive; the one-modulus reduction of $\mathcal{L}_0$ is a flagged model choice.